Nonlinearity 4 (1991) 861–902. Printed in the UK

Coupled arrays of Josephson junctions and bifurcation of maps with S_N symmetry

D G Aronson†, Martin Golubitsky‡ and Martin Krupa§

† School of Mathematics, University of Minnesota, Minneapolis, MN 55455, USA
‡ Department of Mathematics, University of Houston, Houston, TX 77204-3476, USA
§ Department of Mathematics, University of Gröningen, 9700 Av. Gröningen, The Netherlands

Received 1 August 1990, in final form 5 March 1991
Accepted by D A Rand

Abstract. Recently models describing the dynamics of large arrays of Josephson junctions coupled through a variety loads have been studied. Since, in applications, these systems are to be operated in a state of stable synchronous oscillation, these studies have emphasized how the synchronous periodic state can lose stability. A common feature of the models equations is that they are invariant under permutation of the individual junctions. In our study we focus on the effects that these symmetries have on the resulting bifurcations when the synchronous solution loses stability.

In these systems the causes for loss of stability are: fixed-point bifurcations and period-doubling bifurcations. Moreover, these two bifurcations can coalesce in a new codimension-two bifurcation which we call a homoclinic twist bifurcation. Due to the S_N symmetry, it can be shown that the fixed-point bifurcations must lead to families of unstable periodic orbits. The period-doubling bifurcations, however, can lead to stable period-doubled oscillations, and the possible states and their stabilities are classified. In particular, generically, all of the period-doubled oscillations are described by dividing the junctions into two or three groups within which the junctions oscillate synchronously. The existence of these states in the model equations have been confirmed by numerical simulation.

In addition to these period-doubled states, the existence of the homoclinic twist bifurcation and periodic solutions where the junctions oscillate with the same waveform but $(1/N)$th of a period out of phase with each other is observed in the numerical simulation. These last types of solution are called ponies on a merry-go-round (POMS). In these equations POMS do not arise from a local bifurcation. This issue is discussed in the companion paper.

AMS classification scheme numbers: 58F22, 58F14, 34C25

1. Introduction

In a recent series of papers Hadley, Beasley and Wiesenfield [11–13] have studied numerically the dynamics of large series arrays of current biased Josephson junctions coupled through various loads. In applications such as microwave generators and parametric amplifiers it is desirable to operate these circuits at a stable synchronous (i.e. in-phase) oscillation. Thus it is of interest to determine where in parameter space the synchronous oscillations are stable and how the stability is lost. In this paper we focus on the types of states which are produced through bifurcation as the synchronous oscillation loses stability. A common feature of the models considered by Hadley *et al* is that the junctions are all equally coupled to one another through the load so that the equations describing their dynamics are invariant under permutation of the junctions. Thus, in addition to the usual dynamical systems and numerical methods, we can also apply group theoretic methods to the analysis of these arrays. We are therefore able to obtain a rather complete picture of the primary bifurcation structure associated with the in-phase oscillations.

In section 2 we describe the models studied by Hadley *et al* and give a detailed preliminary analysis of the stability of the in-phase oscillations for the two simplest examples of loads (the purely capacitive and purely resistive cases). In particular, we show how the in-phase oscillations are born in a homoclinic connection and how they can lose stability only through a fixed-point or a period-doubling bifurcation. Numerical computations carried out in [12, 13] show that both types of bifurcations do indeed occur for a wide variety of loads, and this is born out by more detailed numerical investigations of the pure capactive and pure resistive load cases (cf figures 6 and 9 below).

The S_N symmetry of the equations governing the evolution of an array of N Josephson junctions is inherited by the Poincaré map associated with the in-phase oscillations. In sections 3, 4, and 5 we study generic S_N symmetric fixed-point and period-doubling bifurcations for maps. Since the S_N-symmetry largely determines the qualitative features of the normal form of these maps near their bifurcations, we are able to obtain a considerable amount of information from this abstract formulation. Specifically, we classify all of the possible symmetry breaking period-two states which can arise in generic S_N-symmetric period-doubling bifurcation (section 3), and discuss their stability (section 4). In section 5 we use recent results of Field and Richardson [8] to discuss briefly the generic fixed-point symmetry-breaking bifurcation. It follows from a result in [14] that generically this bifurcation produces only unstable fixed points.

We emphasize that the analysis in sections 3, 4 and 5 is for generic S_N symmetry-breaking bifurcations. It therefore applies not only to all of the models considered by Hadley *et al,* but also to any system with the appropriate symmetry. On the other hand, for any particular system the analysis tells us only which states cannot occur and which states are possible. Further information can only be obtained by detailed analysis of the particular system. Nevertheless, these abstract results provide an essential framework for studying the dynamics of any system with S_N-symmetry.

In terms of Josephson junction arrays, the results of sections 3, 4 and 5 can be summarized as follows. At a period-doubling bifurcation the period-two points of the Poincaré map correspond to states where the junctions divide into two or three groups. Inside each group the junctions oscillate in phase. When the number of junctions in each group is different, the oscillations associated with each group are distinct and the periods of these oscillations are approximately twice the period of the original synchronous solution. When two of the groups are of the same size, both groups follow the same waveform, but there is a half period phase shift between the groups. If, in addition, there is a third group of oscillators, then generically its size will differ from that of the two equal groups, and its period of oscillation will be half that of the other groups. That is, some of the junctions have period doubled oscillations while others do not.

To determine the stability of each of the possible period-two points requires detailed calculations. The structure imposed on the normal form by the S_N-symmetry makes it possible for us to carry out some of these calculations and determine whether or not a given period-two point can be asymptotically stable. Roughly speaking, the only period two points which can be asymptotically stable are those that correspond to two groups of junctions of approximately equal size. More precisely, if the groups consist of k and $N-k$ junctions, then stability is possible when $N/3 \leqslant k \leqslant N/2$. There are some exceptions to this rule which are described in section 4.

As noted above, the generic S_N-symmetric fixed-point bifurcation produces only asymptotically unstable points. Generically, for each k between 1 and $N/2$, the fixed-point bifurcation produces fixed points in which the junctions are divided into two groups of k and $N-k$ junctions. Within each group the junctions oscillate synchronously. There are no other fixed points.

To supplement our theoretical results, we used numerical simulations to explore the regions of instability of the in-phase periodic solution for junction arrays with capacitive and resistive loads. These results are given in section 6. As predicted, we found no stable periodic solutions resulting from the fixed-point bifurcation. For the resistive load we did find that the period-doubling bifurcation leads to stable period-doubled periodic solutions whose symmetries are consistent with the results of sections 3 and 4. For the capacitive load we found no evidence of stable period-doubled periodic solutions (though this too is consistent with the theory), but we did find stable periodic solutions which are discrete travelling waves. These solutions, which we call *ponies on a merry-go-round*, are discussed more fully in section 6 and are proved to exist using topological methods in the companion paper [3].

In our numerical investigations we also found a new codimension two bifurcation in the capacitive load case at a point on the curve in parameter space along which the homoclinic connections which give rise to the in-phase solutions occur. This point is a *homoclinic twist point* since, roughly speaking, as the parameters are varied along the curve of homoclinic points through it, the tangent flow along the homoclinic trajectory begins to twist vectors in transverse directions. In addition, curves of fixed-point and of period-doubling bifurcation intersect at this codimension-two point. For this reason we call this point a *homoclinic twist bifurcation point.* For the resistive load case there are homoclinic twist points, but no homoclinic twist bifurcations. The existence of these points is discussed in section 2 and they are analysed more fully in section 7.

2. Josephson junction models

We begin this section with a general discussion of the dynamics of two specific circuits discussed in [11–13]. The general circuit considered by Hadley *et al* is shown in figure 1. Let φ_k $(k=1,\ldots,N)$ denote the difference in the phases of the

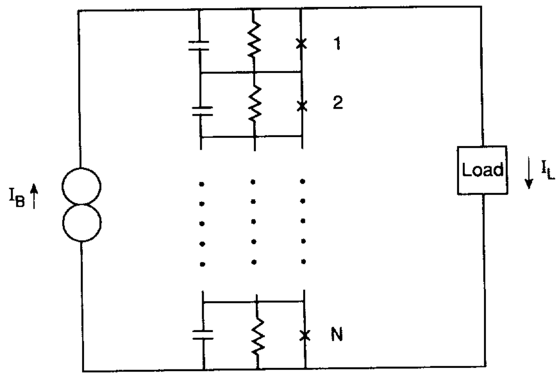

Figure 1. Schematic diagram of a series array of N Josephson junctions with bias current I_B. I_L is the current flowing through the load.

quasiclassical superconducting wavefunctions on the two sides of the kth junction, and let I_L denote the current flowing through the load. Then the evolution of the φ_k and I_L is governed by the system of equations:

$$\beta\ddot{\varphi}_k + \dot{\varphi}_k + \sin(\varphi_k) + I_L = I \tag{2.1a}$$

$$\sum_{j=1}^{N} \dot{\varphi}_j = \mathscr{F}(I_L) \tag{2.1b}$$

where β is a dimensionless measure of the capacitence of the junctions, I_B is the applied bias current, and $\mathscr{F}(\cdot)$ is an integro-differential operator which depends on the particular load considered. Note that the system (2.1) is invariant under permutation of the φ_k.

2.1. Pure capacitive load

When the load is a capacitor equation (2.1b) takes the form:

$$\sum_{j=1}^{N} \dot{\varphi}_j = \frac{1}{C}\int^t I_L \, \mathrm{d}\tau.$$

Following [12, 13] we scale by taking $C = 3/N$ and eliminate I_L from equation (2.1a) to obtain

$$\beta\ddot{\varphi}_k + \dot{\varphi}_k + \sin(\varphi_k) - \frac{3}{N(3+\beta)}\sum_{j=1}^{N}(\dot{\varphi}_j + \sin(\varphi_j)) = \frac{\beta}{3+\beta} I \tag{2.2}$$

for $k = 1, \ldots, N$. Symmetric in-phase solutions to (2.2) are characterized by

$$\varphi_1 = \varphi_2 = \ldots = \varphi_N = \varphi$$

where φ satisfies the 'pendulum equation'

$$(3+\beta)\ddot{\varphi} + \dot{\varphi} + \sin(\varphi) = I. \tag{2.3}$$

Rewrite (2.3) as a first-order system:

$$\begin{aligned} \dot{\varphi} &= \psi \\ \dot{\psi} &= \frac{1}{3+\beta}(I - \sin(\varphi) - \psi). \end{aligned} \tag{2.4}$$

For $I \leqslant 1$ the system (2.4) has rest points at $(\varphi^{\pm}, 0)$, where

$$\varphi^- = \sin^{-1}(I) \qquad \text{and} \qquad \varphi^+ = \pi - \varphi^-.$$

In fact for $I < 1$, $(\varphi^-, 0)$ is a sink and $(\varphi^+, 0)$ is a saddle. For $I = 1$, $\varphi^+ = \varphi^- = \pi/2$ and $(\pi/2, 0)$ is a saddle-node.

In order to study the dynamics of (2.4) it is more convenient to rewrite it in terms of a scaled time variable $\tau = t/\sqrt{3+\beta}$. Then $\Phi(\tau) \equiv \varphi(\sqrt{3+\beta}\,\tau)$ and $\Psi(\tau) \equiv \sqrt{3+\beta}\,\psi(\sqrt{3+\beta}\,\tau)$ satisfy the standard damped driven pendulum system

$$\begin{aligned} \Phi' &= \Psi \\ \Psi' &= I - \sin\Phi - \varepsilon\Psi \end{aligned} \tag{2.5}$$

where $' = \mathrm{d}/\mathrm{d}\tau$ and

$$\varepsilon = 1/\sqrt{3+\beta}.$$

Note that $\varepsilon \leqslant 1/\sqrt{3} < 1$ for $\beta \geqslant 0$. As long as $\Psi \neq 0$, any trajectory $(\Phi(\tau), \Phi(t))$ of (2.5) can be written, with a slight abuse of notation, in the form $\Psi = \Psi(\Phi; \varepsilon, I)$, where

$$\frac{\mathrm{d}\Psi}{\mathrm{d}\Phi} = \frac{1}{\Psi}(I - \sin(\Phi)) - \varepsilon. \tag{2.6}$$

Let $\Psi = \Psi^{\mathrm{u}}(\Phi; \varepsilon, I)$ denote the branch of the unstable manifold from $(\varphi^+, 0)$ which enters the upper half plane for $\Phi > \varphi^+$ when $I < 1$, or the centre unstable manifold from the saddle-node $(\pi/2, 0)$ for $I = 1$. This curve first meets the Ψ'-null cline

$$\Psi = \frac{1}{\varepsilon}(I - \sin(\Phi)) \tag{2.7}$$

at a point with coordinates $(\Sigma^{\mathrm{u}}(\varepsilon, I), \Theta^{\mathrm{u}}(\varepsilon, I))$, where

$$3\pi/2 < \Sigma^{\mathrm{u}}(\varepsilon, I) < \varphi^- + 2\pi$$

and

$$\Theta^{\mathrm{u}}(\varepsilon, I) \equiv \Psi^{\mathrm{u}}(\Sigma^{\mathrm{u}}(\varepsilon, I); \varepsilon, I)$$

(cf figure 2). The branch $\Psi = \Psi^{\mathrm{s}}(\Psi; \varepsilon, I)$ of the stable manifold from $(\varphi^+ + 2\pi, 0)$ which enters the upper half plane for $\Phi < \varphi^+ + 2\pi$ does not necessarily intersect the

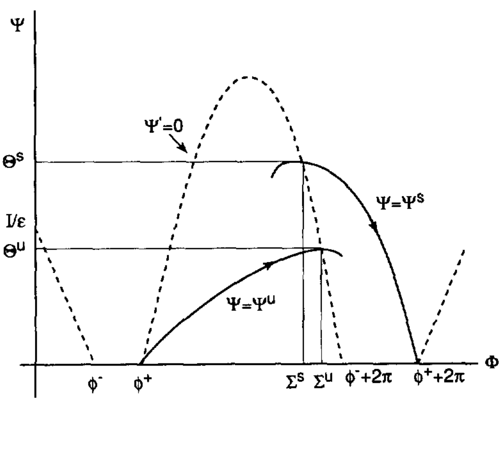

Figure 2. The phase plane for (2.5) with $I < 1$.

Ψ'-null cline, but if it does the first intersection occurs at a point $(\Sigma^s(\varepsilon, I), \Theta^s(\varepsilon, I))$ where $3\pi/2 < \Sigma^s < \varphi^- + 2\pi$ and

$$\Theta^s(\varepsilon, I) \equiv \Psi^s(\Sigma^s(\varepsilon, I); \varepsilon, I)$$

(cf figure 2). Note that the Ψ'-null cline is monotone decreasing on $[3\pi/2, \varphi^- + 2\pi] \subset [3\pi/2, 5\pi/2]$.

We will show that the non-constant symmetric in-phase solutions to (2.2) are generated by homoclinic connections which occur at points in the parameter plane where

$$\Theta^u(\varepsilon, I) = \Theta^s(\varepsilon, I).$$

We begin by establishing the existence of the homoclinic connections.

Consider first the case $I = 1$. At the saddle-nodes $(\Phi, \Psi) = ((4k+1)\pi/2, 0)$ the differential of the right-hand side of (2.5) is

$$\begin{pmatrix} 0 & 1 \\ 0 & -\varepsilon \end{pmatrix}$$

so that $\varepsilon = 0$ is a degerate saddle-node (Takens–Bogdanov point). For $\varepsilon = 0$ we can solve (2.5) by quadrature. The trajectories from the saddle-node at $(\pi/2, 0)$ are given by

$$\Psi = \Psi^{\pm}(\Phi) \equiv \left\{2\left[\Phi - \frac{\pi}{2} - \sin\left(\Phi - \frac{\pi}{2}\right)\right]\right\}^{1/2}$$

and the phase portrait is as shown in figure 3.

For $\varepsilon > 0$ the eigenvalues of the linearized system at the saddle-nodes are 0 and $-\varepsilon$, and the slopes of the corresponding eigenvectors are respectively 0 and $-\varepsilon$. As is easily checked using (2.6), the branch W^s of the stable manifold from $(5\pi/2, 0)$ which enters the upper half-plane for $\Phi < 5\pi/2$ lies below the line

$$\Psi = \Psi^*(\Phi) \equiv \varepsilon\left(\frac{5\pi}{2} - \Phi\right)$$

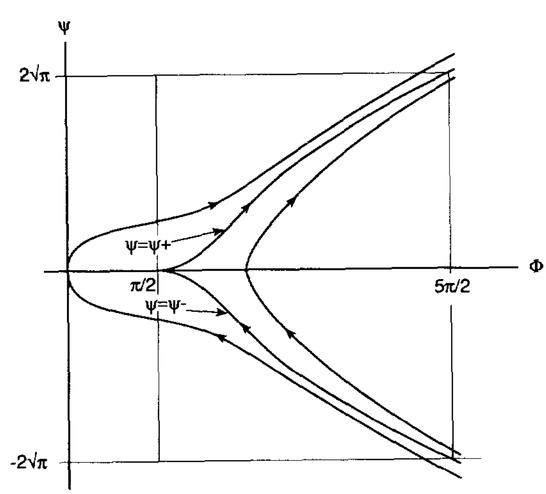

Figure 3. The phase plane for (2.5) with $I = 1$ and $\varepsilon = 0$.

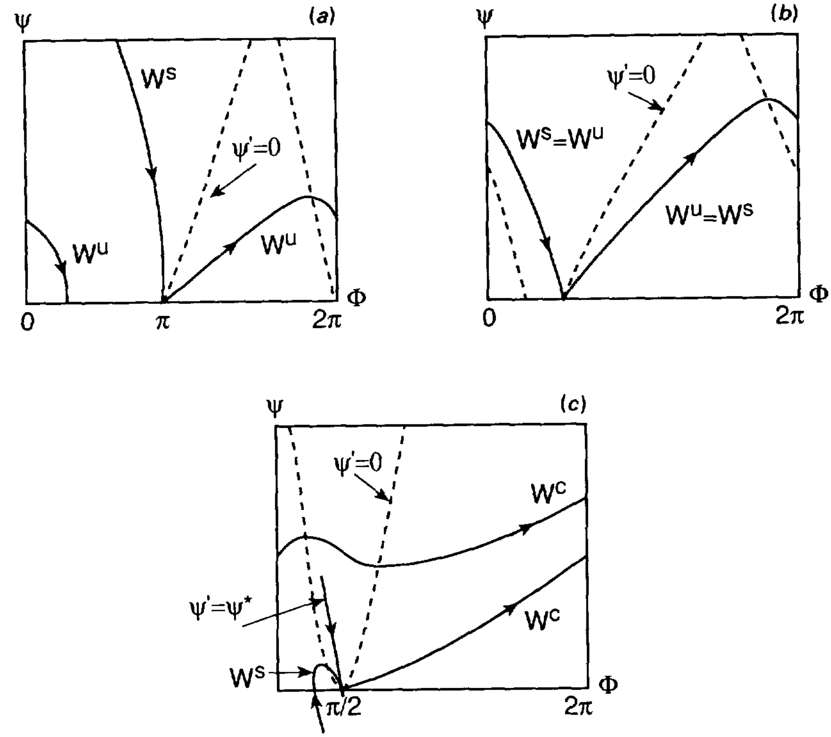

Figure 4. The phase plane for (2.5) for various values of $I \in [0, 1]$ and $\varepsilon > 0$. (a) $I = 0$, $\varepsilon > 0$; $\Theta^u < \infty = \Theta^s$. ($b$) $I \in (0, 1)$, $\varepsilon > 0$; $\Theta^u = \Theta^s$. (c) $I = 1$, $\varepsilon > 0$; $\Theta^u > \Theta^s$.

(cf figure 4(c) in which Φ is reduced modulo 2π). The first intersection Θ^s of W^s with the Ψ'-null cline (2.7) lies below the intersection of $\Psi = \Psi^*(\Phi)$ with this null cline. Thus $\Theta^s(\varepsilon, 1) = O(\varepsilon^2)$. On the other hand, the centre unstable manifold W^c from $(\pi/2, 0)$ stays close to $\Psi = \Psi^+(\Phi)$ and so $\Theta^u(\varepsilon, 0)$ is $O(1)$. Therefore $\Theta^u(\varepsilon, 1) > \Theta^s(\varepsilon, 1)$ and there is no connection. Strictly speaking, in the absence of careful estimates, this argument is valid only for $0 < \varepsilon \ll 1$. However, our numerical investigations show clearly that the conclusions hold for all $\varepsilon \leqslant 1/\sqrt{3}$, i.e. for all $\beta \geqslant 0$. Consequently, we will avoid unessential estimates and simply assume that

$$\Theta^u(\varepsilon, 1) > \Theta^s(\varepsilon, 1) \qquad \text{for all } \varepsilon \leqslant 1/\sqrt{3}. \tag{2.8}$$

At the other extreme, for $I = 0$ the system (2.5) describes an undriven pendulum which is undamped for $\varepsilon = 0$ and damped for $\varepsilon > 0$. In the undamped case $\varepsilon = 0$ there is a homoclinic orbit from the saddle point at $(\pi, 0)$, while in the damped case $\varepsilon > 0$ the pendulum always winds down to the rest state at the origin. Thus for $\varepsilon > 0$ the phase portrait is as shown in figure 4(a).

For each $\varepsilon > 0$, in order to go continuously from the configuration for $I = 0$ shown in figure 4(a) to the configuration for $I = 1$ shown in figure 4(c) there is necessarily at least one value of $I \in (0, 1)$ for which W^s and W^u coincide as shown in figure 4(b). We will show that for each $\varepsilon > 0$ the value of I for which the homoclinic connection occurs is unique and that the resulting function $I = \hat{I}(\varepsilon)$ is continuous. The key result is the following technical lemma.

Lemma 2.1. If $I_1 < I_2$ then

$$\Psi^u(\cdot; \varepsilon, I_1) < \Psi^u(\cdot; \varepsilon, I_2) \qquad \text{on } [\varphi_2^+, \infty) \tag{2.9a}$$

as long as $\Psi^u(\cdot; \varepsilon, I_1) > 0$ and

$$\Psi^s(\cdot; \varepsilon, I_1) > \Psi^s(\cdot; \varepsilon, I_2) \qquad \text{on } (-\infty, \varphi_1^+ + 2\pi) \tag{2.1b}$$

as long as $\Psi^s(\cdot; \varepsilon, I_2) > 0$ (cf figure 5).

Proof. Let $(\varphi_j^\pm, 0)$ denote the rest points of (2.5) with $I = I_j$ and $\Psi_j^u(\Phi) = \Psi^u(\Phi; \varepsilon, I_j)$ for $j = 1, 2$. Since $\varphi_2^+ < \varphi_1^+$ we have $\Psi_2^u > 0$ on $(\varphi_2^+, \varphi_1^+]$ and hence $\Psi_2^u > \Psi_1^u$ for all sufficiently small $\Phi > \varphi_1^+$. Suppose there exists a $\varphi^* > \varphi_1^+$ such that

$$\Psi_2^u > \Psi_1^u \text{ on } (\varphi_1^+, \varphi^*) \qquad \text{and} \qquad \Psi_2^u(\varphi^*) = \Psi_1^u(\varphi^*).$$

Then

$$\frac{\Psi_2^u(\varphi^*) - \Psi_2^u}{\varphi^* - \Phi} < \frac{\Phi_1^u(\varphi^*) - \Psi_1^u}{\varphi^* - \Phi} \qquad \text{on } (\varphi_1^+, \varphi^*)$$

which implies

$$\frac{d}{d\Phi} \Psi_2^u(\varphi^*) \leqslant \frac{d}{d\Phi} \Psi_1^u(\varphi^*).$$

On the other hand,

$$\frac{d}{d\Phi} \Psi_2^u(\varphi^*) = \frac{I_2 - \sin \varphi^*}{\Psi_2^u(\varphi^*)} - \varepsilon = \frac{I_2 - \sin \varphi^*}{\Psi_1^u(\varphi^*)} - \varepsilon > \frac{I_1 - \sin \varphi^*}{\Psi_1^u(\varphi^*)} - \varepsilon = \frac{d}{d\Phi} \Psi_1^u(\varphi^*)$$

yields a contradiction. Thus we conclude that (2.9a) holds as long as $\Psi_1^u > 0$. The proof of (2.9b) is similar and we omit it. □

An immediate consequence of the lemma is the following.

Corollary 2.2. For each fixed $\varepsilon \in (0, 1/\sqrt{3}]$, $\Theta^u(\varepsilon, I)$ is an increasing function of I and $\Theta^s(\varepsilon, I)$ is a decreasing function of I.

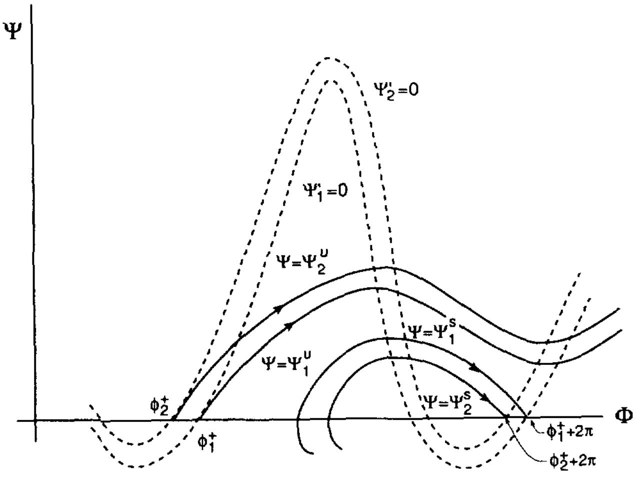

Figure 5. The phase plane for (2.5). $\Psi_j' = \Psi'(\Phi; \varepsilon; I_j)$ for $j = 1, 2$.

From the corollary we conclude that for each $\varepsilon \in (0, 1/\sqrt{3}]$ there exists a unique $\hat{I}(\varepsilon) \in (0, 1)$ such that

$$\Theta^{u}(\varepsilon, I) < \Theta^{s}(\varepsilon, I) \qquad \text{for } 0 \leqslant I < \hat{I}(\varepsilon) \tag{2.10a}$$

$$\Theta^{u}(\varepsilon, I) = \Theta^{s}(\varepsilon, I) \qquad \text{for } I = \hat{I}(\varepsilon) \tag{2.10b}$$

$$\Theta^{u}(\varepsilon, I) > \Theta^{s}(\varepsilon, I) \qquad \text{for } \hat{I}(\varepsilon) < I \leqslant 1. \tag{2.10c}$$

Let

$$G \equiv \{(\varepsilon, I) : \varepsilon \in (0, 1/\sqrt{3}], I = \hat{I}(\varepsilon)\} \subset (0, 1/\sqrt{3}) \times (0, 1).$$

If $(\varepsilon_1, I_1) \in G^c$ then $\Theta^{u}(\varepsilon_1, I_1) \neq \Theta^{s}(\varepsilon_1, I_1)$ and it follows from standard continuity results for ordinary differential equations that this inequality holds for all (ε, I) in some neighbourhood of (ε_1, I_1). Therefore G is closed. Now let $\{\varepsilon_k\}$ be any sequence in $(0, 1/\sqrt{3}]$ such that $\varepsilon_k \rightarrow \varepsilon_0 \in (0, 1/\sqrt{3}]$ and

$$I_0 \equiv \lim_{k \to \infty} \hat{I}(\varepsilon_k)$$

exists. Then, since G is closed, $(\varepsilon, I_0) \in G$ and, by uniqueness, $I_0 = \hat{I}(\varepsilon_0)$. Therefore $\hat{I}(\varepsilon)$ is continuous on $(0, 1/\sqrt{3}]$. Moreover, it is not difficult to show that $\hat{I}(\varepsilon) \rightarrow 0$ as $\varepsilon \downarrow 0$.

To summarize our results we return to the original parameter $\beta = \varepsilon^{-2} - 3$. We have shown that there exists a continuous curve $I = I(\beta)$ in the first quadrant of the (β, I)-parameter plane such that $I(\beta) \rightarrow 0$ as $\beta \rightarrow \infty$, $0 < I(\beta) < 1$ for $0 \leqslant \beta < \infty$, and such that at each parameter point $(\beta, I(\beta))$ the stable and unstable manifolds of the saddle point $(\varphi^+, 0)$ coincide $(\mathrm{mod}\, 2\pi)$ as shown in figure 4(*b*). Figure 6 shows the curve $I = I(\beta)$ as computed using AUTO.

For $I \in [0, I(\beta))$ almost all trajectories of (2.4) are attracted $(\mathrm{mod}\, 2\pi)$ to the sink at $(\varphi^-, 0)$. For $I \in (I(\beta), 1]$ the homoclinic connection is broken and, in view of (2.10) the phase portrait for (2.4) is as shown in figure 7(*a*). In particular, the closed segment $[a, I + 1]$ of the line $\varphi = 0$ is mapped $(\mathrm{mod}\, 2\pi)$ by the flow into its open interior so that there is a fixed point which corresponds to a symmetric in-phase running solution. The same fixed point argument works for $I > 1$ since, as seen in figure 7(*b*), the flow maps $(\mathrm{mod}\, 2\pi)$ the closed segment $[0, I + 1]$ into its open interior. Thus, for any (β, I) with $I > I(\beta)$ there exists a symmetric in-phase

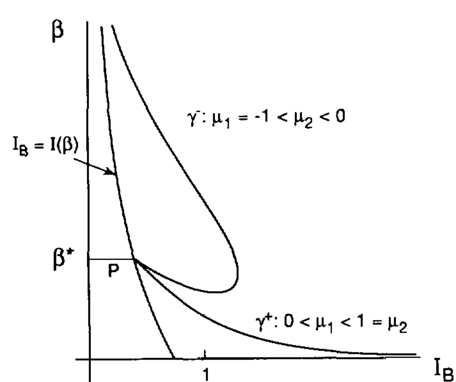

Figure 6. The (I, β) parameter plane for (2.4). The curve of homoclinic connections is $I = I(\beta)$. γ^- indicates the curve of period-doubling bifurcations and γ^+ indicates the curve of fixed-point bifurcations. The point labelled P is the codimension-two homoclinic twist bifurcation point. This figure is based on computations done using AUTO.

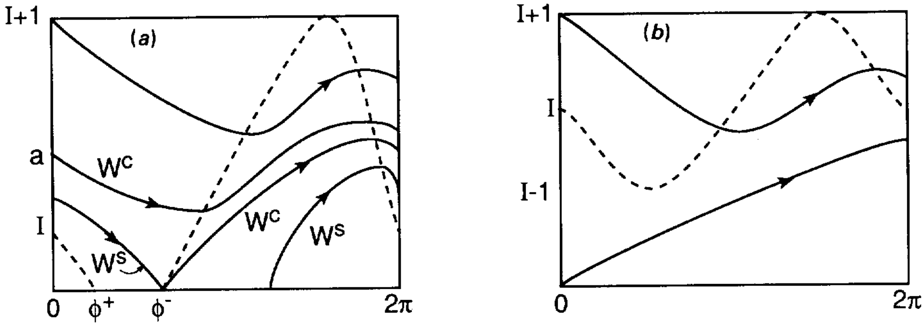

Figure 7. The phase plane for (2.4) at various values of I. (a) $I(\beta) < I \leqslant 1$. (b) $I > 1$.

running solution. Moreover, as the following argument shows, this running solution is unique. Note that for $I \in (I(\beta), 1$, the running solution coexists with the sink $(\varphi^-, 0)$.

The variational equation for (2.4) is

$$\dot{X} = \begin{pmatrix} 0 & 1 \\ -\dfrac{\cos\varphi}{3+\beta} & -\dfrac{1}{3+\beta} \end{pmatrix} X. \tag{2.11}$$

If φ is a running solution to (2.4) with period T, i.e. if

$$\varphi(t+T) = \varphi(t) + 2\pi$$

then the corresponding Floquet multipliers λ_1 and λ_2 satisfy

$$\lambda_1 \lambda_2 = \mathrm{e}^{-T/(3+\beta)}.$$

However, since $X = \dot{\varphi}$ is a periodic solution to (2.11), one of the multipliers, say λ_1, equals 1. Thus

$$0 < \lambda_2 = \mathrm{e}^{-T/(3+\beta)} < 1$$

and we conclude that *every running solution to* (2.4) *is stable as an object in the* (φ, ψ)*-plane,* but not necessarily as an object in the full $2N$-dimensional phase space. Consequently, there can be at most one in-phase running solution for any parameter point (β, I).

We now turn to the question of the stability of the symmetric in-phase running solution φ of (2.2) as a solution in the full $2N$-dimensional phase space. The first variation of φ_k about φ satisfies the linear system

$$\beta\ddot{\zeta}_k + \dot{\zeta}_k + \zeta_k \cos(\varphi) + \frac{3}{N(3+\beta)} \sum_{j=1}^{N} (\dot{\zeta}_j + \zeta_j \cos(\varphi)) = 0$$

for $k = 1, \ldots, N$. To analyse this system it is convenient to use the variables

$$\eta_k = \zeta_{k+1} - \zeta_k \qquad (k = 1, \ldots, N-1)$$

$$\vartheta = \frac{1}{N} \sum_{j=1}^{N} \zeta_j.$$

In these variables the variational system is

$$(3+\beta)\ddot{\theta} + \dot{\theta} + \theta\cos(\varphi) = 0$$

$$\beta\ddot{\eta}_k + \dot{\eta}_k + \eta_k\cos(\varphi) = 0 \qquad (k = 1, \ldots, N-1)$$

or, written as a first-order system,

$$\dot{\xi} = \mathscr{A}(t)\xi$$

where $\mathscr{A}(t)$ is the block diagonal matrix

$$\mathscr{A}(t) = \begin{pmatrix} A(t) & & & 0 \\ & B(t) & & \\ & & \ddots & \\ 0 & & & B(t) \end{pmatrix}$$

with

$$A(t) = \frac{1}{3+\beta}\begin{pmatrix} 0 & 3+\beta \\ -\cos(\varphi) & -1 \end{pmatrix} \qquad B(t) = \frac{1}{\beta}\begin{pmatrix} 0 & \beta \\ -\cos(\varphi) & -1 \end{pmatrix}.$$

As we have seen, the Floquet multipliers corresponding to $A(t)$ are $\lambda_1 = 1$ and $\lambda_2 = e^{-T/(3+\beta)}$. Thus the stability of φ depends on the multipliers μ_1 and μ_2 of the remaining blocks $B(t)$ which occur with multiplicity $N-1$. By Abel's theorem

$$\mu_1\mu_2 = e^{-T/\beta}.$$

Thus either μ_1 and μ_2 are complex conjugates on the circle of radius $e^{-T/2\beta} < 1$, or else they are both real and of the same sign. In particular, *the only possible bifurcations from φ are either fixed point* $(0 < \mu_1 < \mu_2 = 1)$ *or period doubling* $(-1 = \mu_1 < \mu_2 < 0)$.

Computations show that in the present purely capacitive load case both fixed point and period doubling bifurcations actually occur. Figure 6 shows the computationaly derived curves γ^+ of fixed point bifurcation and γ^- of period doubling bifurcation. The bifurcation curves γ^+ and γ^- interesect at a point $P \equiv (\beta^*, I(\beta^*))$ on the homoclinic connection curve $I = I(\beta)$. The symmetric in-phase rotation is stable for parameter points in the region to the right of the curves γ^+ and γ^-. For parameter points (β, I) between $I = I(\beta)$ and γ^- we have

$$\mu_1 < -1 < -e^{-T/\beta} < \mu_2 < 0$$

with $\mu_1 \to -\infty$ as $(\beta, I) \to (\tilde{\beta}, I(\tilde{\beta}))$ for $\tilde{\beta} > \beta^*$. Similarly,

$$0 < \mu_1 < e^{-T/\beta} < 1 < \mu_2$$

for parameter points (β, I) between $I = I(\beta)$ and γ^+ with $\mu_2 \to \infty$ as $(\beta, I) \to (\tilde{\beta}, I(\tilde{\beta}))$ for $0 \leq \tilde{\beta} < \beta^*$. The codimension two point P where γ^+, γ^- and Γ intersect is the homoclinic twist bifurcation point mentioned above. We will discuss it in more detail in section 7 and in [2].

2.2. Pure resistive load

In another model considered by Hadley *et al* [12, 13] the load is a resistor and equation (2.1*b*) is simply

$$\sum_{j=1}^{N} \dot{\varphi} = RI_L.$$

Following [12] we scale by taking $R = N$ and eliminate I_L from equation (2.1*a*) to obtain

$$\beta\ddot{\varphi}_k + \dot{\varphi}_k + \sin(\varphi_k) + \frac{1}{N}\sum_{j=1}^{N} \dot{\varphi}_j = I \tag{2.12}$$

for $k = 1, 2, \ldots, N$. Symmetric in-phase solutions to (2.12) satisfy

$$\beta\ddot{\varphi} + 2\dot{\varphi} + \sin(\varphi) = I. \tag{2.13}$$

Rewrite (2.13) as a system

$$\begin{aligned} \dot{\varphi} &= \psi \\ \dot{\psi} &= \frac{1}{\beta}(I - \sin(\varphi) - \psi). \end{aligned} \tag{2.14}$$

For $I \leqslant 1$, this system has the same rest points at $(\varphi^{\pm}, 0)$ as the corresponding system in the purely capacitive case (2.4).

For large β the dynamics of solutions to (2.14) are quite similar to those of solutions to (2.4). However, for small β the situation is different since (2.14) becomes singular as $\beta \downarrow 0$. In the singular limit $\beta = 0$ we have the 'slow' dynamics which take place on the $\dot{\psi}$-null cline and are given by

$$\psi = (I - \sin(\varphi))/2 \qquad \dot{\varphi} = \psi.$$

For $0 < \beta \ll 1$ we also have the 'fast' dynamics off the ψ-null cline characterized by $\dot{\psi} = \mathrm{O}(1/\beta)$.

For $0 < \beta \ll 1$ all trajectories of (2.14) very quickly relax to a small neighbourhood of the $\dot{\psi}$-null cline, and the phase portrait with $I = 1$ is as shown in figure 8(*a*). The centre unstable manifold W^{c} of the saddle-node $(\pi/2, 0)$ is forced back into the saddle-node (mod 2π) by the fact that the stable manifold W^{s} is almost vertical. Thus for $I = 1$ and $0 < \beta \ll 1$ there is a homoclinic orbit (saddle-node/saddle-node connection).

For $\beta \gg 1$ an analysis similar to the analysis of the capacitive load case carried out in subsection 2.1 shows that there is no homoclinic connection and that the phase portrait is as shown in figure 8(*c*). In order to have a continuous transition from the configuration in figure 8(*a*) with a homoclinic connection and the configuration in figure 8(*c*) with no connection there must be at least one critical value of β for which the stable manifold W^{s} and the centre unstable manifold W^{c} coincide (figure 8(*b*)). Our simple geometric arguments are not sufficiently strong to prove the uniqueness of the critical value of β. The difficulty arises from the fact that (in the notation of subsection 2.1) both $\Theta^{\mathrm{u}}(\varepsilon, 1)$ and $\Theta^{\mathrm{s}}(\varepsilon, 1)$ are increasing functions of $\varepsilon = 2/\sqrt{\beta}$ so that more detailed estimates are needed in order to establish transversality. We will not attempt to do thus here but will rely on our numerical studies which show that *there is a unique critical value $\hat{\beta}$ of β for which W^{s} and W^{c} coincide.*

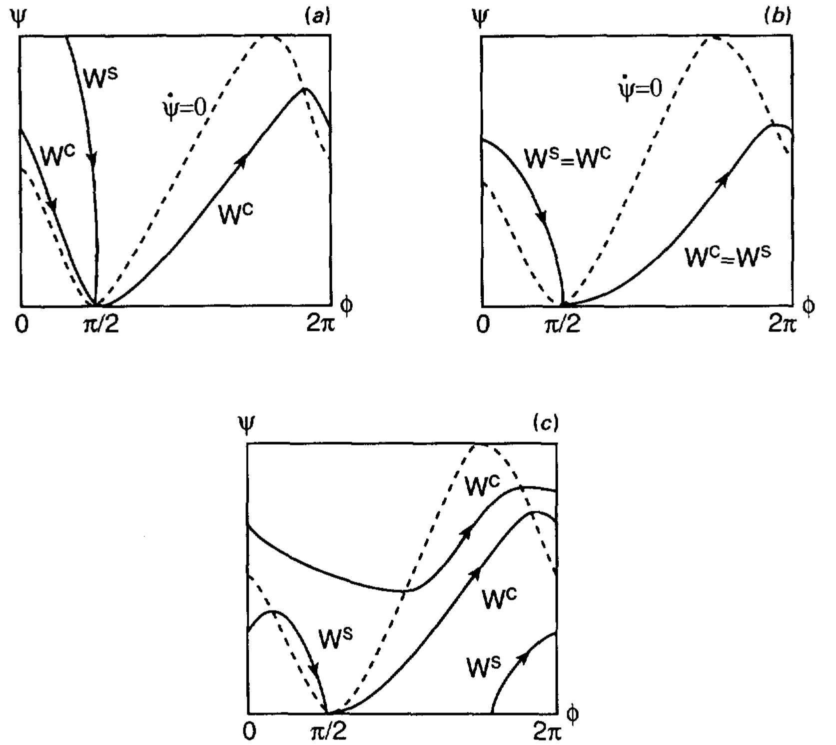

Figure 8. The phase plane for (2.14) for $I=1$ and various values of β. (a) $I=1$, $0<\beta\ll 1$. (b) $I=1$, β critical. (c) $I=1$, $\beta\gg 1$.

For $\beta>\hat{\beta}$ we can repeat the analysis of subsection 2.1 to establish the existence of a continuous curve $I=I(\beta)$ along which the homoclinic connection occurs, where $0<I(\beta)<1$ for $\hat{\beta}<\beta<\infty$, $I(\beta)\to 0$ as $\beta\to\infty$, and $I(\beta)\to 1$ as $\beta\to\hat{\beta}$. We extend the definition of $I(\beta)$ by setting $I(\beta)\equiv 1$ for $0<\beta\leqslant\hat{\beta}$. Schecter [16] has shown that $I'(\hat{\beta}+0)=0$ so that the extended curve $I=I(\beta)$ is smooth for $\beta\geqslant 0$. Figure 9 shows the curve $I=I(\beta)$ as computed using AUTO.

As in the case of the capacitive load, for $I\in[0, I(\beta))$ almost all trajectories of (2.13) are attracted $(\mathrm{mod}\, 2\pi)$ to the sink at $(\varphi^-, 0)$. For $I\in(I(\beta), \infty)$, after the homoclinic connection is broken, the arguments given in subsection 2.1 can be repeated here to establish the existence of a unique symmetric in-phase running solution φ which, moreover, is asymptotically stable in the (φ, ψ)-phase plane (cf figure 7).

The stability analysis for the symmetric in-phase running solution φ in the full $2N$-dimensional phase space is completely analogous to the corresponding analysis for (2.2). The result is again that only fixed-point or period-doubling bifurcations can occur. Careful numerical studies involving both direct calcualtion of Floquet multipliers and continuations using AUTO, show that both period doubling and fixed point bifurcations occur in this case just as in the capacitive load case. Figure 9 shows the computationally derived curve γ^- of period doubling bifurcations along which the multipliers μ_1 and μ_2 of $\dot{y}=B(t)y$ satisfy $-1=\mu_1<\mu_2<0$, and the curve γ^+ of fixed point bifurcations along which $0<\mu_1<\mu_2=1$. Note that both γ^+ and γ^- intersect $I=I(\beta)$ on its vertical part, i.e., for $\beta\in(0, \hat{\beta})$. Several striking differences

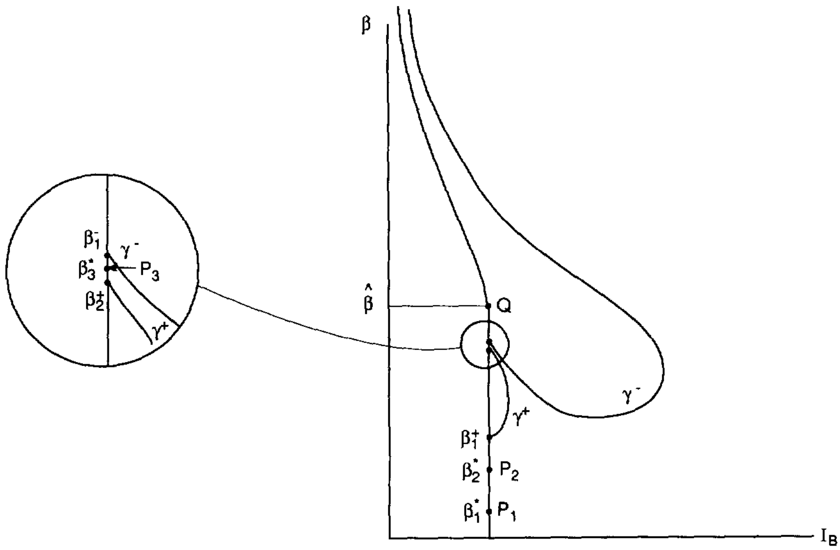

Figure 9. The (I, β)-parameter plane for (2.14). The curve of homoclinic connections is given by $I=1$ below point Q, and by $I=I(\beta)$ above it. γ^- indicates the curve of period-doubling bifurcations and γ^+ indicates the curve of fixed-point bifurcations. The points labelled P_j for $j=1,2,3$ are homoclinic twist points. The points with coordinates $(1, \beta_1^-)$, $(1, \beta_1^+)$ and $(1, \beta_2^+)$ are bifurcation points. This figure is based on computations done using AUTO.

between the capacitive and resistive load cases should be noted. As we observed above, in the capacitive load case the bifurcation curves γ^+ and γ^- intersect at a point $(I(\beta^*), \beta^*)$ on the homoclinic birth curve Γ, and this intersection point is a homoclinic twist point. In the resistive load case γ^+ intersects Γ at $(1, \beta_1^+)$ and $(1, \beta_2^+)$ while γ^- intersects Γ at $(1, \beta_1^-)$, where

$$0 < \beta_1^+ < \beta_2^+ < \beta_1^-.$$

In particular, γ^+ and γ^- do not intersect on Γ although their intersections $(1, \beta_2^+)$ and $(1, \beta_1^-)$ with Γ are very close together. Also these bifurcation points are not homoclinic twist points although there is a homoclinic twist point on Γ in the interval (β_2^+, β_1^-) and two more on Γ in the interval $(0, \beta_1^+)$.

Roughly speaking, the bifurcations do not occur at the homoclinic twist points here as they do in the capacitive load case because of the difference in the behavior of the Floquet multipliers on a running solution near a saddle-node/saddle-node connection or near a saddle/saddle connection. We return to this question briefly in section 7 and in more detail in [2]. Finally we note that in the resistive load case with $\beta = 0$ both of the Floquet multipliers for the running solution are equal to one [17].

3. Period doubling with S_n symmetry

As we indicated in section 1, many models of coupled arrays of n Josephson junctions lead, for certain parameters, to a loss of stability of the synchronous (in-phase) periodic solution where Floquet multipliers go through -1, that is, by a period doubling bifurcation. Moreover, in the cases that have been studied, these multipliers, due to the permutation symmetry of the array models, have multiplicity $n-1$.

In this section we study abstractly the question of symmetry-breaking period doubling bifurcations. As we noted in the introduction this information is needed to set the framework for the study of bifurcation in models for large arrays of coupled oscillators. These general results will be used to interpret the numerical results we describe in section 6. We do this by studying period doubling for generic S_n-equivariant mappings on the $(n-1)$-dimensional eigenspace V corresponding to the critical Floquet multiplier. This S_n-equivariant mapping is obtained from the original problem by a centre manifold reduction applied to the Poincaré mapping of the synchronous periodic solution.

Our main results (theorems 3.1–3.4) enumerate all of the period two points which occur for the generic S_n-equivariant mapping at such a period doubling bifurcation, with a small exception when n is divisible by three. We begin by giving a precise description of V and the action of S_n on V.

Let the permutation group S_n act on $\mathbb{R}^n$ by permuting the axes and let

$$V=\{(x_1,\ldots,x_n)\in\mathbb{R}^n : x_1+\ldots+x_n=0\}. \tag{3.1}$$

The subspace V is invariant and absolutely irreducible under S_n. In this section we discuss period doubling of mappings on V that are S_n equivariant. Thus we let

$$g: V\times\mathbb{R}\to V$$

be smooth and assume

$$g(\sigma x,\lambda)=\sigma g(x,\lambda) \tag{3.2}$$

for all permutations σ. Let I_V be the identity map on V. Absolute irreducibility implies

$$g(0,\lambda)=0 \tag{3.3a}$$

$$(dg)_{0,\lambda}=c(\lambda)I_V. \tag{3.3b}$$

By a *period doubling* bifurcation at $\lambda=0$ we mean

$$c(0)=-1. \tag{3.4}$$

We consider the situation where the invariant fixed point $x=0$ is asymptotically stable when $\lambda<0$ and loses stability at $\lambda=0$, that is,

$$c'(0)<0 \tag{3.5}$$

Then, the eigenvalues of $(dg)_{0,\lambda}$ have modulus less than unity for negative λ. It may easily be checked that assumptions (3.1)–(3.5) are (generically) valid for the Josephson junction models we study.

The question we address is: what are the period-two points that arise generically from this period doubling bifurcation? The approach we use is the one in [6], which we now describe. We assume that g is transformed to a normal form f by a near identity transformation up to whatever finite order is needed. That is, we assume that

$$f: V\times\mathbb{R}\to V$$

is $S_n \times \mathbb{Z}_2$ equivariant, where $\mathbb{Z}_2 = \{\pm I_V\}$. For such an f, period two points are found by solving the equation

$$f(x, \lambda) = -x. \tag{3.6}$$

The oddness of f insures that solutions x to (3.6) are period two points of f. Assuming (3.5), the equivariant branching lemma [10, theorem XIII, 3.3] implies that there is a unique branch of period two points solving (3.6) for each isotropy subgroup $\Sigma \subseteq S_n \times \mathbb{Z}_2$ satisfying

$$\dim \mathrm{Fix}(\Sigma) = 1 \tag{3.7}$$

where

$$\mathrm{Fix}(\Sigma) = \{y \in V : \sigma y = y \; \forall \sigma \in \Sigma\}.$$

Such Σ satisfying (3.7) are *maximal* isotropy subgroups of $S_n \times \mathbb{Z}_2$.

Whether solutions to (3.6) exist with submaximal isotropy is a difficult question; at present each situation must be handled on a case-by-case basis.

Once the existence of period two points for f is established, there is a general method for proving the existence of corresponding period-two points for the S_n-equivariant mapping g. This proof is accomplished in two parts:

(i) analyse f to the order in which the period-two points of f are generically hyperbolic,

(ii) assume this hyperbolicity holds (i.e. that the genericity hypotheses are valid) and use the implicit function theorem or normal hyperbolicity to prove the existence for g. See [6], theorem 4.1.

In this section we

(i) classify all isotropy subgroups of $S_n \times \mathbb{Z}_2$, up to conjugacy,

(ii) determine all maximal isotropy subgroups with one-dimensional fixed point subspaces, and

(iii) determine which submaximal isotropy subgroups support period-two solutions to (3.6).

The isotropy subgroups for the action of $S_n \times \mathbb{Z}_2$ on V divide naturally into two classes: subgroups of S_n and subgroups of $S_n \times \mathbb{Z}_2$ not in S_n. The first case leads to subgroups defined as follows: partition n into s blocks with the jth block having k_j elements. Thus

$$k_1 + \ldots + k_s = n. \tag{3.8}$$

Then the isotropy subgroup associated with these s blocks is

$$\Sigma_k \equiv S_{k_1} \times S_{k_2} \times \ldots \times S_{k_s} \tag{3.9a}$$

where

$$\dim \mathrm{Fix}(\Sigma_k) = s - 1. \tag{3.9b}$$

In the application to large arrays of Josephson junctions, the blocks mentioned above correspond to groupings of synchronous oscillators.

To define the second class, partition n into $2r + 1$ blocks. Pair the blocks so that the $(2j - 1)$th and the $(2j)$th blocks each have l_j members and the last block has l_{r+1} members. Thus

$$2l_1 + \ldots + 2l_r + l_{r+1} = n. \tag{3.10}$$

Define

$$T_l \equiv S_{l_1} \times S_{l_1} \times \ldots \times S_{l_r} \times S_{l_r} \times S_{l_{r+1}} \times \mathbb{Z}_2(\rho_l) \tag{3.11a}$$

where

$$\dim \mathrm{Fix}(T_l) = r \tag{3.11b}$$

and ρ_l is an order-two group element defined as follows. Consider the jth pair of blocks consisting of members

$$a_1, \ldots, a_{l_j} \qquad \text{and} \qquad b_1, \ldots, b_{l_j}$$

respectively. Define the permutation

$$\rho^j = (a_1, b_1) \cdot \ldots \cdot (a_{l_j}, b_{l_j}) \tag{3.12a}$$

$$\rho_l = (\rho^1 \cdot \ldots \cdot \rho^r, -I) \in S_n \times \mathbb{Z}_2. \tag{3.12b}$$

The fact that $-I$ appears in the symmetry ρ_l implies that the periodic solutions corresponding to the two blocks have the same waveform but are a half-period out of phase.

Theorem 3.1. The conjugacy classes of isotropy subgroups of $S_n \times \mathbb{Z}_2$ acting on V are given by:

(*a*) Σ_k where $k = (k_1, \ldots, k_s)$ satisfies (3.8) and $s \geqslant 2$ except when $s = 2$ and $k_1 = k_2$. We may also assume

$$k_1 \leqslant \ldots \leqslant k_s.$$

(*b*) T_l where $l = (l_1, \ldots, l_{r+1})$ satisfies (3.10) and $r \geqslant 1$. We may also assume

$$l_1 \leqslant \ldots \leqslant l_r.$$

That Σ_k and T_l are isotropy subgroups can be seen by computing their fixed point subspaces:

$$\mathrm{Fix}(\Sigma_k) = \{(y_1, \ldots, y_s) \in V: \\ y_j = c_j(1, \ldots, 1) \in \mathbb{R}^{k_j} \quad \text{for some scalar } c_j\} \tag{3.13a}$$

$$\mathrm{Fix}(T_l) = \{(z_1, -z_1, \ldots, z_r, -z_r, 0) \in V: \\ z_j = c_j(1, \ldots, 1) \in \mathbb{R}^{l_j} \quad \text{for some scalar } c_j\} \tag{3.13b}$$

Now take any point in $\mathrm{Fix}(\Sigma)$ where the $|c_j|$'s are distinct; then the isotropy of that point is exactly Σ. This choice of c_j is possible except in the case $s = 2$ and $k_1 = k_2$. It follows that the dimensions of the fixed point subspaces are those given in (3.9*b*) and (3.11*b*). The proof of theorem 3.1—that these are the only isotropy subgroups—will be given below.

We can now answer the second question.

Corollary 3.2. The conjugacy classes of isotropy subgroups of $S_n \times \mathbb{Z}_2$ acting on V having one-dimensional fixed point subspaces are:

$$\Sigma_k = S_k \times S_{n-k} \qquad 1 \leqslant k < \frac{n}{2} \tag{3.14a}$$

$$T_l = S_l \times S_l \times S_{n-2l} \times \mathbb{Z}_2(\rho_l) \qquad 1 \leqslant l \leqslant \frac{n}{2}. \tag{3.14b}$$

Moreover, these are all of the maximal isotropy subgroups of $S_n \times \mathbb{Z}_2$. Note that $S_0 = S_1 = \{1\}$.

Apply theorem 4.1 of [2] to conclude that a period doubling bifurcation with S_n symmetry produces unique branches of period-two solutions for each isotropy subgroups Σ_k and T_l.

Next we show that generically period-two solutions with submaximal isotropy do not exist for many isotropy subgroups.

Theorem 3.3. (*a*) Generically isotropy subgroups of the form T_l where $r > 1$ have no solutions.

(*b*) Generically isotropy subgroups Σ_k where $k = (k_1, k_1, n - 2k_1)$ have no solutions.

(*c*) Generically isotropy subgroups of the form Σ_k where $s \geqslant 4$ have no solutions.

Let

$$F = f \mid \mathrm{Fix}(\Sigma) \times \mathbb{R}.$$

We shall prove (*a*) by showing that solutions to $F(x, \lambda) = -x$ must have isotropy larger than T_l if $r > 1$, and (*c*) by showing that such solutions must have isotropy larger than Σ_k when $s \geqslant 4$. We do this using explicit calculations with the general $S_n \times \mathbb{Z}_2$ equivariant restricted to appropriate fixed point subspaces. We prove (*b*) by counting the number of period two solutions with maximal isotropy that must exist in $\mathrm{Fix}(\Sigma_k)$ by theorem 3.1. Then we show that generically this number is the maximum number of solutions that occur in $\mathrm{Fix}(\Sigma_k)$. Hence no solutions with submaximal symmetry occur generically with this isotropy.

Theorem 3.4. The isotropy subgroups Σ_{k_1,k_2,k_3}, where the k_j are distinct, support period-two solutions. These solutions are determined at third order unless one k_j is the average of the other two.

By 'support solutions' we mean that generically there exist branches of solutions emanating from the period doubling bifurcation. This theorem is proved in two ways. First we use topological degree arguments to prove the existence of period-two points with submaximal symmetry. Second, we use explicit calculations to show that when $k_2 \neq (k_1 + k_3)/2$ these submaximal solutions are determined at third order. These calculations are used in section 4 to determine asymptotic stability.

The remainder of this section is devoted to the proof of theorems 3.1, 3.3 and 3.4.

We begin with some general remarks. Let Γ be a finite group acting on a space V and suppose that $-I_V \notin \Gamma$. Then $\Gamma \times \mathbb{Z}_2$ acts on V. Let $\Sigma \subset \Gamma \times \mathbb{Z}_2$ be a proper isotropy subgroup and let $K = \Sigma \cap \Gamma$.

Lemma 3.5. Under these assumptions:

(*a*) K is an isotropy subgroup for Γ acting on V.

(*b*) Either $\Sigma = K \subset \Gamma$ or the index of K in Σ is two.

(*c*) In the second case there is an element $h \in \Gamma \sim K$ such that

$$\Sigma = (K, I_V) \cup (Kh, -I_V). \tag{3.15}$$

Proof. The proofs of (b) and (c) follow from lemma 4.2 of [6].

(a) Since Σ is a proper isotropy subgroup of the action of $\Gamma \times \mathbb{Z}_2$ on V, Σ must fix some non-zero vector x. It follows that K fixes x. If some element γ of Γ fixes x, then γ is in Σ, since Σ is the isotropy subgroup of x. Hence $\gamma \in K$ and K is the isotropy subgroup of x in Γ. □

Proof of theorem 3.1. The isotropy subgroups of S_n acting on V are known (cf [8]) and they are the subgroups listed in (3.9a), with the single exception that the case $s=2$, $k_1=k_2$ is also an isotropy subgroup of S_n. We note, however, that Σ_{k_1,k_1} is not an isotropy subgroup of $S_n \times \mathbb{Z}_2$ since Σ_{k_1,k_1} fixes $(x, -x)$, but so does $(x, y) \to -(y, x)$. Thus the isotropy subgroups of $S_n \times \mathbb{Z}_2$ lying inside S_n are precisely those listed in theorem 3.1(a).

Now let Σ be an isotropy subgroup of $S_n \times \mathbb{Z}_2$ that is not in S_n. It follows from lemma 3.5 that

$$\Sigma = (K, I_V) \cup (Kh, -I_V)$$

where $K \subset S_n$ is an isotropy subgroup and h is a permutation satisfying $h^2 \in K$. Since K is an isotropy subgroup of S_n, we can partition the set $\{1, \ldots, n\}$ into s blocks with K having the form, up to conjugacy, of (3.9a).

Now write the permutation h as a product of disjoint cycles and omit from h any cycle permutating members of a single block; this amounts to choosing another element in the coset Kh. We assert that we can choose h to be a product of disjoint transpositions.

To prove this assertion we first observe that h^2 cannot be in K if h contains a cycle of odd length. This follows since such a cycle must permute elements in at least two different blocks and its square, which has the same length, must also; hence its square is not in K. Since h is a product of disjoint cycles, all of these cycles commute. Thus, h^2 is not in K, since h^2 is the product of the squares of each of the cycles of h. Suppose now that h contains a cycle of even length greater than two; without loss of generality we may assume that this cycle is $p=(1, 2, \ldots, 2m)$, where $m>1$. Note that $p^2=p_1 \cdot p_2$ where $p_1=(1, 3, \ldots, 2m-1)$ and $p_2=(2, 4, \ldots, 2m)$. Since $p^2 \in K$, we must have that $1, 3, \ldots, 2m-1$ and $2, 4, \ldots, 2m$ are in the same blocks. Hence $p_1, p_2 \in K$. We now replace h by $p_1^{-1} \cdot p = (1, 2) \cdot (3, 4) \cdot \ldots \cdot (2m-1, 2m)$. Consequently we can assume that h is a product of disjoint 2-cycles, as asserted. Thus, $h^2=1$. (This fact is not valid for general groups Γ.)

Next we assert that if h permutes members of two blocks, then these blocks must be of equal size; moreover, h must interchange all members of these blocks. To prove this assertion, we use the fact that Σ is an isotropy subgroup. Suppose that Σ fixes $x \in \mathbb{R}^n$. Since K is the isotropy subgroup of x in S_n (theorem 3.1(a)), we may asssume that K has the form:

$$K = S_{k_1} \times S_{k_2} \times \ldots \times S_{k_s}.$$

Hence,

$$x = (c_1, \ldots, c_1, \ldots, c_s, \ldots, c_s)$$

where the c_j's are all distinct. Now we know that h is a product of transpositions that interchange elements of different blocks. Suppose that h contains a 2-cycle that interchanges element of the first two blocks. Since $(h, -I) \in \Sigma$, it follows that

$c_2 = -c_1$ and that c_1 is non-zero (else c_2 and c_1 would not be distinct). Observe that for h to fix x it is necessary that h map every element of the first block to an element of the second block, since h must map a position containing a c_1 to a position containing a c_2 and all of the c_2's are in the second block (since again the c_j's are all distinct). Similarly, h must map all of the entries in the second block to the first block. Thus, the first block and the second block have the same number of elements. After renumbering, this proves the assertion; hence, we may assume that h contains all cycles in (3.12a).

Finally, we know that h must permute a fixed number of pairs of blocks, say r. Thus ρ_l defined by (3.12b) is in the isotropy subgroup Σ. It follows that the vector x fixed by K has the form:

$$x = (c_1, \ldots, c_1, c_2, \ldots, c_2, \ldots, c_{2r}, \ldots, c_{2r}, \ldots)$$

where

$$c_2 = -c_1, \ldots, c_{2r} = -c_{2r-1}.$$

For such an x to be fixed by ρ_l we must have all of the remaining entries equal to zero. The isotropy subgroup fixing such an x has the form T_l where

$$l_j = k_{2j} \text{ for } j = 1, \ldots, r \text{ and } l_{r+1} = n - 2(l_1 + \ldots + l_r).$$

To discuss the existence of period-two points with submaximal isotropy we need to write out the general $S_n \times \mathbb{Z}_2$ equivariant mapping. The form of these mappings may be derived directly from the form of the general S_n equivariant mapping, which is known. We summarize here the results which may be found in [8, §9]. Let

$$\sigma_j(x) \equiv x_1^j + \ldots + x_n^j \tag{3.16a}$$

$$X_j \equiv \frac{1}{j+1} \pi_V \nabla \sigma_{j+1} \mid V = (x_1^j, \ldots, x_n^j) - \frac{\sigma_j}{n}(1, \ldots, 1) \tag{3.16b}$$

where $\pi_V : \mathbb{R}^n \to V$ is orthogonal projection. Then:

Proposition 3.6. (a) The set $\{\sigma_2, \ldots, \sigma_n\}$ forms a Hilbert basis for the S_n invariant polynomials on V.

(b) The set $\{X_1, \ldots, X_{n-1})$ forms a free basis for the module of S_n equivariant polynomial mappings over the ring of S_n invariant polynomials.

Consequently, the S_n equivariant mapping $g : V \times \mathbb{R} \to V$ can be written uniquely in the form

$$g(x, \lambda) = p_1(x) X_1(x) + \ldots + p_{n-1}(x) X_{n-1}(x)$$

where the p_j are functions of $\sigma_2, \ldots, \sigma_n$ and λ.

The $S_n \times \mathbb{Z}_2$ invariant theory follows directly from proposition 3.6, and is summarized by:

Lemma 3.7. (a) The set

$$\{\sigma_j : j \text{ even}; j \leqslant n\} \cup \{\sigma_i \sigma_j : i, j \text{ odd}; 2 \leqslant i, j \leqslant n\}$$

is a Hilbert basis for the $S_n \times \mathbb{Z}_2$ invariant polynomials on V.

(b) The set

$$\{X_j : j \text{ odd}; 1 \leqslant j \leqslant n-1\} \cup \{\sigma_i X_j : i \text{ odd}, j \text{ even}; 3 \leqslant i \leqslant n, 1 \leqslant j \leqslant n-1\}$$

is a basis for the module of $S_n \times \mathbb{Z}_2$ equivariant mappings on V over the ring of $S_n \times \mathbb{Z}_2$ invariant polynomials.

It now follows that up to third order we can write out explicitly the normal form mapping f, namely,

$$f(x, \lambda) = (-1 + \alpha\lambda + \beta\sigma_2)x + \gamma X_3(x) + \dots \tag{3.17a}$$

where

$$X_3(x) = (x_1^3, \dots, x_n^3) - \frac{\sigma_3}{n}(1, \dots, 1). \tag{3.17b}$$

So, remarkably, for all n there exist only two independent $S_n \times \mathbb{Z}_2$ equivariant cubic mappings on V. This fact drastically simplifies the calculations that follow.

Proof of theorem 3.3. (*a*) We let $\Sigma = T_l$ and assume that $r > 1$. We note that $\mathrm{Fix}(\Sigma)$ has the form

$$\mathrm{Fix}(\Sigma) = \{(y_1, -y_1, y_2, -y_2, \dots, y_r, -y_r, 0) : y_j \in \mathbb{R}^{l_j} \text{ is a multiple of } (1, \dots, 1)\}.$$

By abuse of notation we let these multiples be y_j. Since $\mathrm{Fix}(\Sigma)$ is an invariant subspace for f we can write the restriction F in the y_j coordinates. This calculation is simplified by the observation that $\sigma_j \mid \mathrm{Fix}(\Sigma) = 0$ for all odd j. Using lemma 3.7 we arrive at the following explicit expression for $F(y_1, \dots, y_r, \lambda)$

$$p_1 y + p_3 X_3 + \dots + p_{2t+1} X_{2t+1}$$

where $t = [(n-1)/2]$, the p_j are functions of σ_i (i even) and λ, and

$$X_j(y) = (y_1^j, \dots, y_r^j).$$

Thus, solving $F(y, \lambda) = -y$ leads to the system of equations

$$p_1 y_j + p_3 y_j^3 + \dots + p_{2t+1} y_j^{2t+1} = 0 \tag{3.18}$$

for $j = 1, \dots, r$. Observe now that if a solution $(y_1, \dots, y_r, \lambda)$ to (3.18) has some $y_j = 0$, then that solution has isotropy strictly larger than T_l. Thus, we may divide (3.18) by y_j when searching for solutions with isotropy T_l.

We also observe that if a solution has $y_i = \pm y_j$ then the isotropy of that solution is strictly larger than T_l. Next, subtract equations (3.18) for $j = 1$ and 2 (which we can do if $r > 1$), obtaining:

$$(y_1^2 - y_2^2)(p_3 + \dots) = 0. \tag{3.19}$$

Thus, it follows from (3.19) that if $p_3(0) = \gamma$ is non-zero—which generically it is—then solutions to (3.18) must satisfy $y_1 = \pm y_2$. Thus T_l does not support solutions.

(*b*) We begin by observing that the isotropy subgroup $\Sigma = \Sigma_k$ has a two-dimensional fixed point subspace

$$\mathrm{Fix}(\Sigma) = \{(a, \dots, a, b, \dots, b, c, \dots, c) : k_1 a + k_1 b + k_3 c = 0\}$$

where $k_3 = n - 2k_1$ and

$$D(\Sigma) \equiv N(\Sigma)/\Sigma \cong \begin{cases} D_2 & \text{if } k_1 \neq k_3 \\ D_6 & \text{if } k_1 = k_3 \end{cases}$$

where $N(\Sigma)$ is the normalizer of Σ in $S_n \times \mathbb{Z}_2$. Points in $\mathrm{Fix}(\Sigma)$ have isotropy larger than Σ when

$$\{a=b\} \qquad \{a=c\} \qquad \{b=c\} \qquad \{b=-a,\ c=0\},$$

and, in addition, if $k_1=k_3$ when

$$\{c=-a,\ b=0\} \qquad \text{and} \qquad \{c=-b,\ a=0\}.$$

The idea of the proof is the following. Since $-I_V$ is in $S_n \times \mathbb{Z}_2$ it follows from theorem 3.1 that there must be at least eight half branches of period-two solutions emanating from the bifurcation (excluding the trivial fixed point) if $k_1 \neq k_3$ and twelve half branches if $k_1=k_3$.

Recall that equivariance implies that $\mathrm{Fix}(\Sigma)$ is an invariant subspace for f and let $F=f \mid \mathrm{Fix}(\Sigma)\times\mathbb{R}$. Now the restriction F commutes with the action of the group $D(\Sigma)\equiv N(\Sigma)/\Sigma$ on $\mathrm{Fix}(\Sigma)$ where $N(\Sigma)$ is the normalizer of Σ in $S_n\times\mathbb{Z}_2$ (cf lemma XIII, 10.2 in [10]).

Next we recall from [9, chapter X] that generically D_2 equivariant bifurcation problems admit at most eight non-trivial half branches, and from [10, XIII, §5] that generically D_6 equivariant bifurcation problems admit at most twelve non-trivial half branches. Moreover, the genericity conditions for the D_2 equivariant case are at third order and for the D_6 case at fifth order. A long but straightforward calculation shows that generically the restriction F satisfies these genericity conditions, and hence (b) is proved.

(c) It follows from proposition 3.6 and lemma 3.7 that f has the form

$$p_1X_1+p_2X_2+\ldots+p_{n-1}X_{n-1}$$

where $p_{2j}(0)=0$. Each coordinate of $F \mid \mathrm{Fix}(\Sigma)$ has the form

$$p_1a+p_2(a^2-\sigma_2/n)+\ldots+p_{n-1}(a^{n-1}-\sigma_{n-1}/n). \tag{3.20}$$

When $s\geqslant 4$ $F \mid \mathrm{Fix}(\Sigma)$ has at least four coordinates; so we may replace a in (3.20) with b, c, and d, to represent the first four coordinates. We refer to the corresponding formulae as $(3.20)_a$, $(3.20)_b$, etc.

To prove (c) we perform a sequence of calculations. Begin with:

$$\frac{(2.20)_a-(2.20)_b}{a-b}=p_1+p_2\frac{a^2-b^2}{a-b}+\ldots+p_{n-1}\frac{a^{n-1}-b^{n-1}}{a-b} \qquad (3.21)_{a,b}$$

Equation $(3.21)_{a,b}$ is valid if we assume that $a\neq b$. Of course, any solution to $F=0$ that has two equal coordinates has isotropy strictly larger than Σ_k. It follows therefore, that if we want to find solutions with isotropy exactly Σ_k we may assume that $a\neq b$.

Next we assume $a\neq c$ and $b\neq c$ and calculate:

$$\frac{(3.21)_{a,b}-(3.21)_{a,c}}{b-c}$$

$$=p_2\frac{\dfrac{a^2-b^2}{a-b}-\dfrac{a^2-c^2}{a-c}}{b-c}+\ldots+p_{n-1}\frac{\dfrac{a^{n-1}-b^{n-1}}{a-b}-\dfrac{a^{n-1}-c^{n-1}}{a-c}}{b-c} \qquad (3.22)_{a,b,c}$$

Hence, $(3.22)_{a,b,d}$ can be formed if we assume, in addition, that $a\neq d$ and $b\neq d$. Note that the coefficient of p_2 in $(3.22)_{a,b,c}$ reduces to unity and the coefficient of p_3 reduces to $a+b+c$.

Finally, assuming that $c \neq d$ we may calculate:

$$\frac{(3.22)_{a,b,c} - (3.22)_{a,b,d}}{c-d} = p_3 + \ldots = 0. \tag{3.23}$$

It follows from (3.23) that generically no solutions with isotropy Σ_k occur near the period doubling bifurcation, since generically $p_3(0) \equiv \gamma \neq 0$. □

Proof of theorem 3.4. There is a simple degree theoretic proof for the existence of period-two points with submaximal symmetry $\Sigma \equiv \Sigma_{k_1,k_2,k_3}$ where $k_1 < k_2 < k_3$. This proof was pointed out to us (simultaneously) by Pascal Chossat, Mike Field and Ian Melbourne. We need three remarks.

(*a*) $\dim \mathrm{Fix}(\Sigma) = 2$.

(*b*) All of the period-two points with maximal isotropy that lie in $\mathrm{Fix}(\Sigma)$ can be enumerated. There are three branches, one each with isotropy $\Sigma_{k_1+k_2,k_3}$, $\Sigma_{k_2+k_3,k_1}$ and $\Sigma_{k_3+k_1,k_2}$.

(*c*) Each of the bifurcating branches of solutions with maximal isotropy is a pitchfork with the two non-trivial solutions being identified by $-I$.

We have verified (*a*) in (3.9*b*) and (*b*) in corollary 3.4. To verify (*c*) note that $-I$ acts non-trivially on the fixed-point subspaces corresponding to solutions with maximal isotropy.

It follows from (*a*) that the degree of the trivial solution is the same for $\lambda < 0$ and $\lambda > 0$. It follows from (*c*) that the degrees of the two non-trivial solutions of the pitchfork are equal. Assume that there are no solutions with submaximal isotropy. Since the total degree cannot change as λ is varied through zero, it follows that the sum of the degrees of the maximal isotropy solutions is zero. This is impossible since there are three branches of such solutions. □

The calculations in the remainder of this section are needed to show that solutions with submaximal symmetry Σ are determined at third order unless $k_2 = (k_1 + k_3)/2$. We shall need these calculations when we discuss the asymptotic stability of these solutions with submaximal isotropy.

At third order the equations for $F(x, \lambda) = f(x, \lambda) + x = 0$ restricted to $\mathrm{Fix}(\Sigma)$ are:

$$(\alpha\lambda + \beta\sigma_2)a + \gamma(a^3 - \sigma_3/n) = 0 \tag{3.24a}$$

$$(\alpha\lambda + \beta\sigma_2)b + \gamma(b^3 - \sigma_3/n) = 0. \tag{3.24b}$$

Observe that $[(3.24a) - (3.24b)]/(a - b)$ yields:

$$\alpha\lambda + \beta\sigma_2 + \gamma(a^2 + ab + b^2) = 0. \tag{3.25}$$

Any solution to $F = 0$ satisfying $a = b$ has isotropy strictly larger than Σ; so we can assume $a \neq b$. Substituting (3.25) into (3.24*a*) and assuming the genericity condition $\gamma \neq 0$ yields:

$$\sigma_3 = -nab(a + b). \tag{3.26}$$

The proof of this theorem proceeds from the fact that (3.26) is a homogeneous cubic equation. After dividing by b^3 we can write (3.26) in terms of the variable $u = a/b$. From theorem 3.1 we know that there exist solutions to $F = 0$ when $a = b$ and $a = c$. This yields two roots of (3.26), namely,

$$u_1 = -\frac{k_2}{k_1 + k_3} \qquad \text{and} \qquad u_2 = -\frac{k_2 + k_3}{k_1}.$$

Thus, a solution with submaximal isotropy, if it exists, must correspond to the third root of (3.26). This third root is:

$$u_0 = \frac{k_2 - k_3}{k_3 - k_1}. \tag{3.27}$$

Note that a new solution can occur at third order only if u_0 is not equal to one of the other two roots or to $u = 1$ (that is, $a = b$). It is easy to check that when u_0 is equal to 1, u_1 or u_2 one of the k_j equals the average of the other two. Since we assume that this averaging condition does not hold, we see that u_0 leads to a new solution branch at third order.

The actual equation for the branch with submaximal isotropy is obtained by setting $b = u_0 a$ and substituting into (3.27), obtaining:

$$\lambda = -(\phi(k)\beta + \psi(k)\gamma)b^2/\alpha \tag{3.28}$$

where

$$\phi(k) = [k_1(k_2 - k_3)^2 + k_2(k_3 - k_1)^2 + k_3(k_1 - k_2)^2]/(k_3 - k_1)^2$$
$$\psi(k) = [(k_3 - k_1)^2 - (k_3 - k_2)(k_2 - k_1)]/(k_3 - k_1)^2.$$

Note that $\phi(k)$ and $\psi(k)$ are always positive. This branch is supercritical if the coefficient

$$\phi(k)\beta + \psi(k)\gamma > 0.$$

Next we show that the existence of the branch, that we have established at third order, persists independently of what the higher-order terms in F are. Here we use a result of McLeod and Sattinger [15]. See also [4]. This result states that a solution (a, b, λ) to (3.24) persists independently of higher-order terms if the two equations (3.24a) and (3.24b) have independent gradients with respect to (a, b) at the solution (a, b, λ).

These gradients are independent if the determinant of the matrix

$$\begin{pmatrix} -\lambda + \beta\sigma_2 + \beta a\sigma_{2,a} + 3\gamma a^2 - \gamma\sigma_{3,a}/n & a\beta\sigma_{2,b} - \gamma\sigma_{3,b}/n \\ b\beta\sigma_{2,a} - \gamma\sigma_{3,a}/n & -\lambda + \beta\sigma_2 + \beta b\sigma_{2,b} + 3\gamma b^2 - \gamma\sigma_{3,b}/n \end{pmatrix} \tag{3.29}$$

is non-zero. Using (3.25) allows us to rewrite (3.29) as:

$$\begin{pmatrix} a\beta\sigma_{2,a} + \gamma(2a^2 - ab - b^2 - \sigma_{3,a}/n) & a\beta\sigma_{2,b} - \gamma\sigma_{3,b}/n \\ b\beta\sigma_{2,a} - \gamma\sigma_{3,a}/n & b\beta\sigma_{2,b} + \gamma(2b^2 - ab - a^2 - \sigma_{3,b}/n) \end{pmatrix}$$
$$= \frac{\gamma}{n}[\beta\rho + \gamma\tau] \tag{3.30}$$

where

$$\rho = (b - a)[n\sigma_{2,a}a(2b + a) - n\sigma_{2,b}b(2a + b) + \sigma_{2,a}\sigma_{3,b} - \sigma_{2,b}\sigma_{3,a}]$$
$$\tau = (b - a)[n(2a + b)(a + 2b)(a - b) + (a + 2b)\sigma_{3,a} - (2a + b)\sigma_{3,b}].$$

Define:

$$\begin{aligned} K_1 &= (k_2 + k_3 - 2k_1)/(k_3 - k_1) \\ K_2 &= (k_1 + k_3 - 2k_2)/(k_3 - k_1) \\ K_3 &= (k_1 + k_2 - 2k_3)/(k_3 - k_1). \end{aligned} \tag{3.31}$$

Then compute, using $a = u_0 b$ and (3.27), that:

$$\begin{aligned}
\sigma_{2,a} &= -2bk_1K_2\\
\sigma_{2,b} &= 2bk_2K_1\\
\sigma_{3,a} &= 3b^2k_1K_2\\
\sigma_{3,b} &= -3b^2k_2K_1\\
2a+b &= -bK_2\\
a+2b &= bK_1\\
a-b &= bK_3.
\end{aligned} \tag{3.32}$$

It follows that:

$$\begin{aligned}
\rho &= 2b^4K_1K_2K_3[k_1(k_2-k_3)K_2 + k_2(k_1-k_3)K_1]\\
\tau &= b^4K_1K_2K_3[(k_1+k_2-2k_3)^2 + 3k_1^2 + 3k_2^2]/(k_3-k_1).
\end{aligned} \tag{3.33}$$

Hence, generically the gradients of (3.24a,b) are independent if one index is not the average of the other two. The non-degeneracy conditions are $\gamma \neq 0$ and a certain condition involving β and γ that we do not compute explicitly here.

4. Asymptotic stability

In this section we compute the asymptotic stability for the solutions whose existence was demonstrated in the previous section. In general, computing the eigenvalues of an $n \times n$ matrix is quite complicated. Our calculations here are simplified in two ways.

First, as was shown in (3.17), independent of n, there exist only two linearly independent equivariant cubics in the normal form f. This makes explicit calculations using the truncated normal form possible. Recall from (3.17) that the coefficients of these cubics are β and γ.

Second, the decomposition of V into irreducible representations of an isotropy subgroup lets us block diagonalize df when evaluated at a solution with that isotropy. This allows us to show that, independent of n, there are at most three independent eigenvalues of df whose signs are not determined by exchange of stability considerations.

More precisely, for each of the isotropy subgroups Σ_k, T_l and Σ_{k_1,k_2,k_3} we can decompose

$$V = \mathrm{Fix}(\Sigma) \oplus W_1 \oplus W_2 \oplus \ldots \oplus W_t \tag{4.1}$$

where the W_j's are all distinct absolutely irreducible representations of Σ. It then follows that df, evaluated at a solution of (3.6) with isotropy Σ, is a scalar multiple of the identity when restricted to each W_j. We show below that, independent of n, $t \leqslant 3$. Thus, we can determine the eigenvalues of df on Fix(Σ) by exchange of stability considerations, and the eigenvalues whose eigenvectors lie in transverse directions to Fix(Σ) with a minimum of calculation.

In section 3 we assumed that the invariant fixed point $x = 0$ is asymptotically stable when $\lambda < 0$ and loses stability by a period doubling bifurcation at $\lambda = 0$. See (3.4) and (3.5). The assumption of normal form allows us to find period-two points by solving (3.6), which we write as:

$$F(x, \lambda) \equiv f(x, \lambda) + x = 0.$$

In our discussion of stability we actually work with the eigenvalues of dF which, because of isotropy, are real. Thus, near bifurcation, positive eigenvalues of dF correspond to eigenvalues of df inside the unit circle. Hence asymptotic stability of period two points of f—and hence, assuming hyperbolicity, of g—corresponds to *positive* eigenvalues of dF.

Theorem 4.1. Consider period-two solutions ot (3.6) with isotropy $\Sigma_k = S_k \times S_{n-k}$, where $1 \leqslant k < n/2$.

(*a*) When $1 < k < n/3$, these solutions are generically unstable, the genericity condition being $\gamma \neq 0$.

(*b*) When $n/3 < k < n/2$, these solutions are stable if:

$$\gamma > 0 \quad \text{and} \quad nk(n-k)\beta + (n^2 - 3nk + 3k^2)\gamma > 0.$$

(*c*) When $k = n/3$, the stability of these solutions is not determined at third order. Necessary conditions for stability are

$$\gamma > 0 \quad \text{and} \quad 2k\beta + \gamma > 0.$$

In addition, a condition involving fifth-order terms needs to be satisfied in order for stability to hold.

(*d*) When $k = 1$, these solutions are stable if:

$$\gamma < 0 \quad \text{and} \quad n(n-1)\beta + (n^2 - 3n + 3)\gamma > 0.$$

Theorem 4.2. Consider period-two solutions to (3.6) with isotropy $T_l = S_l \times S_l \times S_{n-2l} \times \mathbb{Z}_2(\rho_l)$, where $1 \leqslant l \leqslant [n/2]$.

(*a*)† When $1 \leqslant l < n/2$, these solutions are generically unstable, the genericity condition being $\gamma \neq 0$.

(*b*) When $l = n/2$, these solutions are stable if:

$$\gamma > 0 \quad \text{and} \quad n\beta + \gamma > 0.$$

Theorem 4.3. Consider period-two solutions to (3.6) with isotropy Σ_{k_1,k_2,k_3} where $1 \leqslant k_1 < k_2 < k_3$. These solutions can be asymptotically stable only if:

$$k_1 = 1 \quad \text{and} \quad k_3 < 2k_2 - 1.$$

Moreover, if these conditions hold, then for certain choices of $\gamma > 0$ and β asymptotic stability holds.

The first step in the proofs of these theorems is the explicit computation of the W_j in (4.1).

For the first set of isotropy subgroups Σ_k we have:

$$\begin{aligned} W_1 &= \left\{(x, 0) \in \mathbb{R}^k \times \mathbb{R}^{n-k} : \sum x_j = 0\right\} \\ W_2 &= \left\{(0, y) \in \mathbb{R}^k \times \mathbb{R}^{n-k} : \sum y_j = 0\right\}. \end{aligned} \tag{4.2}$$

† When $l = 1$ and $n = 3$, the stability of T_l solutions is not determined at third order. See [6].

Observe that (4.1) holds with (4.2) except that:

W_1 is omitted when $k=1$.

For the second set of isotropy subgroups T_l we have:

$$\begin{aligned}
W_1 &= \left\{(x, y, 0) \in \mathbb{R}^l \times \mathbb{R}^l \times \mathbb{R}^{n-2l} : \sum x_j = 0 = \sum y_j\right\} \\
W_2 &= \left\{(0, 0, z) \in \mathbb{R}^l \times \mathbb{R}^l \times \mathbb{R}^{n-2l} : \sum z_j = 0\right\} \\
W_3 &= \left\{\left(1, \ldots, 1, \frac{-2l}{n-2l}, \ldots, \frac{-2l}{n-2l}\right) \in \mathbb{R}^{2l} \times \mathbb{R}^{n-2l}\right\}.
\end{aligned} \tag{4.3}$$

Observe that (4.1) holds with (4.3) except that:

W_1 is omitted when $l=1$

W_2 is omitted when $l=[n/2]$

W_3 is omitted when $l=n/2$.

For the third set of isotropy subgroups Σ_{k_1,k_2,k_3} we have:

$$\begin{aligned}
W_1 &= \left\{(x, 0, 0) \in \mathbb{R}^{k_1} \times \mathbb{R}^{k_2} \times \mathbb{R}^{k_3} : \sum x_j = 0\right\} \\
W_2 &= \left\{(0, y, 0) \in \mathbb{R}^{k_1} \times \mathbb{R}^{k_2} \times \mathbb{R}^{k_3} : \sum y_j = 0\right\} \\
W_3 &= \left\{(0, 0, z) \in \mathbb{R}^{k_1} \times \mathbb{R}^{k_2} \times \mathbb{R}^{k_3} : \sum z_j = 0\right\}.
\end{aligned} \tag{4.4}$$

Observe that (4.1) holds with (4.4) except that:

W_1 is omitted when $k_1 = 1$.

The second step is to determine how to compute eigenvalues of df on each W_j. This is a straightforward calculation since $(dF) \mid W_j$ is this eigenvalue times the identity matrix. For example, in the Σ_k case we can choose $v = (1, -1, 0, \ldots, 0) \in W_1$ and compute the corresponding eigenvalue μ. Since

$$\mu v = (dF)(v) = (\partial F_1/\partial x_1 - \partial F_1/\partial x_2, *, \ldots, *)$$

and the first entry of v is 1, we see that

$$\mu = \partial F_1/\partial x_1 - \partial F_1/\partial x_2.$$

Here we assume that $F = (F_1, \ldots, F_n)$ in coordinates. The other cases are similar; we record the results:

$$(\Sigma_k)\begin{cases} W_1 & \partial F_1/\partial x_1 - \partial F_1/\partial x_2 \\ W_2 & \partial F_n/\partial x_n - \partial F_n/\partial x_{n-1} \end{cases} \tag{4.5}$$

$$(T_l)\begin{cases} W_1 & \partial F_1/\partial x_1 - \partial F_1/\partial x_2 \\ W_2 & \partial F_n/\partial x_n - \partial F_n/\partial x_{n-1} \\ W_3 & \partial F_1/\partial x_1 + \ldots + \partial F_1/\partial x_{2l} - \dfrac{2l}{n-2l}(\partial F_1/\partial x_{2l+1} + \ldots + \partial F_1/\partial x_n) \end{cases} \tag{4.6}$$

$$(\Sigma_{k_1,k_2,k_3})\begin{cases} W_1 & \partial F_1/\partial x_1 - \partial F_1/\partial x_2 \\ W_2 & \partial F_{k_2}/\partial x_{k_2} - \partial F_{k_2}/\partial x_{k_2+1} \\ W_3 & \partial F_n/\partial x_n - \partial F_n/\partial x_{n-1} \end{cases} \tag{4.7}$$

In the third step, we take the third-order truncated normal form of F from (3.17), namely,

$$(\alpha\lambda + \beta\sigma_2)x + \gamma X_3(x). \tag{4.8}$$

Then we compute the derivatives listed in (4.5)–(4.7) evaluated on Fix(Σ). Recall that for the isotropy subgroups we consider here, Fix(Σ) is given by the formulae:

$$\begin{aligned} &\mathrm{Fix}(\Sigma_k) = \left\{s\left(1, \ldots, 1, \frac{-k}{n-k}, \ldots, \frac{-k}{n-k}\right) \in \mathbb{R}^k \times \mathbb{R}^{n-k}\right\} \\ &\mathrm{Fix}(T_l) = \{s(1, \ldots, 1, -1, \ldots, -1, 0) \in \mathbb{R}^l \times \mathbb{R}^l \times \mathbb{R}^{n-2l}\} \\ &\mathrm{Fix}(\Sigma_{k_1,k_2,k_3}) = \{(a, \ldots, a, b, \ldots, b, c, \ldots, c) \in \mathbb{R}^{k_1} \times \mathbb{R}^{k_2} \times \mathbb{R}^{k_3}\} \end{aligned} \tag{4.9}$$

It follows from (4.8) that

$$F_j = (\alpha\lambda + \beta\sigma_2)x_j + \gamma(x_j^3 - \sigma_3/n). \tag{4.10}$$

The branches themselves are determined by $F \mid \mathrm{Fix}(\Sigma)$. Here we discuss the first two types of isotropy subgroups. The third was discussed in (3.28). $F \mid \mathrm{Fix}(\Sigma)$ leads to the branching equations:

$$\begin{aligned} &(\Sigma_k) \qquad \alpha\lambda + \beta\sigma_2 + \gamma\frac{n^2 - 3nk + 3k^2}{(n-k)^2}s^2 = 0 \\ &(T_l) \qquad \alpha\lambda + \beta\sigma_2 + \gamma s^2 = 0. \end{aligned} \tag{4.11}$$

Next we compute the derivatives in (4.5) and (4.6). The first derivative, $\partial F_1/\partial x_1 - \partial F_1/\partial x_2$, is:

$$\begin{aligned} &(\Sigma_k) \qquad \frac{n}{(n-k)^2}(2n - 3k)\gamma s^2 \\ &(T_l) \qquad 2\gamma s^2. \end{aligned} \tag{4.12}$$

The second derivative, $\partial F_n/\partial x_n - \partial F_n/\partial x_{n-1}$, is:

$$\begin{aligned} &(\Sigma_k) \qquad -\frac{n}{(n-k)^2}(n - 3k)\gamma s^2 \\ &(T_l) \qquad -\gamma s^2. \end{aligned} \tag{4.13}$$

Proof of theorem 4.1. In order for solutions with Σ_k isotropy to be asymptotically stable we need the eigenvalues listed in (4.12) and (4.13) to be positive. The sign of the eigenvalue in (4.12) is sgn(γ), since k is between 1 and $n/2$. When $\gamma > 0$ the eigenvalue in (4.13) is positive only when $k > n/3$. This proves (*a*).

The eigenvalue corresponding to Fix(Σ) is positive precisely when the branch of period two points is supercritical (exchange of stability). From (4.11) we compute that:

$$\lambda = -\frac{s^2}{\alpha(n-k)^2}[n(n-k)\beta + (n^2 - 3nk + 3k^2)\gamma] + \ldots.$$

Since $\alpha < 0$ by assumption (3.5), this branch is supercritical if

$$n(n-k)\beta + (n^2 - 3nk + 3k^2)\gamma > 0. \tag{4.14}$$

These calculations verify (*b*).

To have stability when $k = n/3$ we still need $\gamma > 0$ and (4.14) to be valid, as in the proof of (*b*). In this case (4.14) reduces to the condition stated in the theorem. The difficulty here is that the eigenvalues in (4.13) are zero to third order and a computation to fifth order is necessary in order to establish stability.

We can see that fifth order suffices as follows. From (4.2) we know that all of the eigenvalues associated with W_2 are equal; so we need compute only one of them. We consider the two-dimensional space $V = \mathrm{Fix}(\Sigma_{\kappa,\kappa,\kappa})$ and observe that the eigenvalue of $\mathrm{d}F \mid V$ transverse to the line $\mathrm{Fix}(\Sigma_k)$ is the eigenvalue associated with W_2. Now $F \mid V \times \mathbb{R}$ commutes with $D(\Sigma_{\kappa,\kappa,\kappa})$, which as noted in the proof of theorem 3.3(*b*) is isomorphic to D_6. Furthermore, period doubling bifurcations with D_6 symmetry are known to produce period two points whose stability is determined (generically) at fifth order (see [6] or [10]). Moreover, the non-degeneracy condition needed to determine stability is precisely the one needed to show that solutions with submaximal $\Sigma_{\kappa,\kappa,\kappa}$ symmetry do not exist. We note that this sign is independent of the conditions on the third-order terms needed for stability.

Finally, we recall that the eigenvalue in (4.12) is omitted when $k = 1$. In this case we are free to choose $\gamma < 0$ to make the eigenvalue in (4.13) positive, thus establishing (*d*). □

Proof of theorem 4.2. By inspection, it is obvious that the eigenvalues in (4.12) and (4.13) are of opposite signs when $\gamma \neq 0$. Thus, when both eigenvalues are present, which occurs in the range $1 < l < [n/2]$, these period-two solutions are unstable. Thus, we have verified (*a*) except when $l = 1$ and $l = (n-1)/2$.

When $l = n/2$, the eigenvalues corresponding to (4.13) and W_3 are to be omitted. The eigenvalue in (4.12) is positive when $\gamma > 0$. Thus stability occurs when the branch is supercritical. From (4.11) we compute the branching equation:

$$\lambda = -\frac{s^2}{\alpha}[n\beta + \gamma] + \dots .$$

Since $\alpha < 0$ by assumption (3.5), supercriticality corresponds to

$$n\beta + \gamma > 0,$$

thus establishing (*b*).

To determine the stability of solutions when $l = 1$ or when $l = (n-1)/2$ we have to compute $\mathrm{d}F$ on W_3, as given in (4.8). We obtain:

$$\begin{aligned} &(l = 1) && 2\frac{n-3}{n}\gamma s^2 \\ &\left(l = \frac{n-1}{2}\right) && -\frac{n-3}{n}\gamma s^2. \end{aligned} \tag{4.15}$$

When $l = 1$, we omit the eigenvalue in (4.13), but the eigenvalues in (4.12) and (4.15) have opposite signs, as long as $n \neq 3$. When $l = (n-1)/2$, we omit the eigenvalue in (4.13), but here the eigenvalues in (4.12) and (4.15) have opposite signs. This completes the verification of (*a*). □

Proof of theorem 4.3. In coordinates we can write F to third order as in (3.24). Computing the derivatives in (4.7) yields the eigenvalues transverse to $\mathrm{Fix}(\Sigma)$. These computations are straightforward if the computations in (3.32) are used. The results are:

$$\begin{array}{ll} (W_1) & -\gamma b^2 K_2 K_3 \\ (W_2) & -\gamma b^2 K_1 K_3 \\ (W_3) & -\gamma b^2 K_1 K_2. \end{array} \tag{4.16}$$

Observe that the assumption $k_1 < k_2 < k_3$ implies that $K_1 > 0$ and $K_3 < 0$ while K_2 can have either sign. In any case, the sign of the eigenvalue in the space W_2 is positive only when $\gamma > 0$, which we now assume. The signs of the eigenvalues in the spaces W_1 and W_3 are now $\mathrm{sgn}(K_2)$ and $-\mathrm{sgn}(K_2)$, respectively. Thus when both eigenvalues are present the solutions are unstable. This happens for all isotropy subgroups except for those for which $k_1 = 1$, when the eigenvalues in W_1 are omitted.

When $k_1 = 1$ the transverse eigenvalues to $\mathrm{Fix}(\Sigma)$ are all positive only if K_3 is negative. Note that $K_3 < 0$ when

$$k_2 < 2k_3 - 1,$$

which we now assume. For these isotropy subgroups we have stable period two points precisely when the eigenvalues of $\mathrm{d}F$ on $\mathrm{Fix}(\Sigma)$ are positive. To compute the signs of these eigenvalues, we need to compute $\det(\mathrm{d}F)$ and $\mathrm{tr}(\mathrm{d}F)$. We already computed $\det(\mathrm{d}F)$ when we computed the determinant in (3.30)—see (3.33). The trace of (3.30) can be computed in a straightforward manner, using the computations in (3.32). We obtain:

$$\mathrm{tr}(\mathrm{d}F) = b^2[2\beta(k_2K_1 - k_1K_2u_0) - 3\gamma(k_1K_2 - k_2K_1)/n] \tag{4.17}$$

Finally, one checks that it is possible to choose $\gamma > 0$ and β so that both $\det(\mathrm{d}F)$ and $\mathrm{tr}(\mathrm{d}F)$ are positive. □

5. Bifurcation of fixed points

As discussed in section 2, loss of stability of the in-phase periodic solutions of the Josephson junction equations can occur either through period doubling or through bifurcation of fixed points. In this section we discuss both existence and stability of bifurcating fixed points for maps with S_n symmetry. These bifurcating fixed points correspond to asymmetric periodic solutions of the ODE with period approximately equal to that of the in-phase solution. Our results are based entirely on the work of Field and Richardson [8] and Ihrig and Golubitsky [14], and lead to the somewhat surprising conclusion that generically all bifurcating fixed points are asymptotically unstable. Indeed, this conclusion is supported by the numerical computations on which we will report in the next section.

A symmetry breaking fixed point bifurcation of the Poincaré map associated with an in-phase S_n-symmetric periodic solution leads after a centre manifold reduction to an S_n-equivariant mapping

$$g: V \times \mathbb{R} \to V$$

where V is the $(n-1)$-dimensional space defined in (3.1). The absolute irreducibility of S_n acting on V implies

$$g(0, \lambda) = 0 \tag{5.1a}$$

$$(\mathrm{d}g)_{0,\lambda} = c(\lambda) I_V. \tag{5.1b}$$

The assumption of a *fixed point* bifurcation of g at $\lambda = 0$ implies

$$c(0) = +1. \tag{5.2}$$

We study the situation where the invariant fixed point $x = 0$ has a generic change in stability at $\lambda = 0$, that is,

$$c'(0) \neq 0. \tag{5.3}$$

Observe that bifurcating fixed points satisfy the equation:

$$f(x, \lambda) \equiv g(x, \lambda) - x = 0 \tag{5.4}$$

with eigenvalues of $(\mathrm{d}f)_{0,\lambda}$ passing through the origin with nonzero speed as λ is varied.

Field and Richardson [8] determine all of the zeros of (5.5) that occur generically at such a bifurcation. They prove that there is a unique branch of bifurcating zeros to each maximal isotropy subgroup of S_n and that each of these subgroups has a one-dimensional fixed-point subspace. These maximal isotropy subgroups were listed previously in (3.14*a*) with the single exception that $k = n/2$ also gives an isotropy subgroup. Thus we can expect $[n/2]$ bifurcating branches of zeros, each corresponding to periodic solutions where the n oscillators divide into two groups with the oscillators in each group behaving identically.

Note that the stability of the bifurcating solutions are determined by the signs of the real part of the eigenvalues of df. Ihrig and Golubitsky [14] show that when there exists a non-zero equivariant quadratic mapping, then generically all branches of bifurcating zeros corresponding to maximal isotropy subgroups with one-dimensional fixed-point subspaces are unstable. Their proof is based on the fact that irreducibility implies that $\operatorname{tr} \mathrm{d}f_2 \equiv 0$ where f_2 is the quadratic part of f, and hence generically there must be eigenvalues of df with real parts of each sign. We have already listed the S_n-equivariants in proposition 3.6. In particular, X_2, as defined in (3.16*b*), is a non-zero quadratic S_n-equivariant mapping.

6. Numerical simulation

In order to test and supplement some of the theoretical predictions made in previous sections concerning period-doubling bifurcations we wrote programs to integrate both the capacitive and resistive loaded Josephson junctions with a variable number of oscillators. The programs were run on an Apollo DN4500 colour system, with the trajectory of each oscillator appearing in a different colour. For each oscillator we plotted the phase φ against $\dot{\varphi}$. The phase was plotted modulo 2π. This made it rather easy to see when a set of oscillators merged into one block (all but one colour disappeared) and when two blocks of oscillators had the same trajectory but were out of phase. A difficulty with this method, however, is that it was impossible to obtain hard copy of the graphical output. In this section we document our results by giving explicit parameter values (β, I, N) and initial conditions for the trajectories we describe. Most simulations were done with two to thirteen oscillators.

6.1. Pure resistive load

We integrated the second-order system (2.2) by writing it as a first-order system:

$$\dot{\varphi}_k = \psi_k \tag{6.1a}$$

$$\dot{\psi}_k = \frac{1}{\beta}\left(I - \psi_k - \sin(\varphi_k) - \frac{1}{N}\sum_{j=1}^{N} \psi_j\right) \tag{6.1b}$$

for $k = 1, \ldots, N$.

As noted in section 2.1, see figure 9, the in-phase periodic solutions are born at homoclinic bifurcations (which can be tracked in the two-dimensional S_N-symmetric phase plane). Since these in-phase periodic solutions are asymptotically stable in this plane, they are easily found.

The numerical evidence presented in [12] indicates that in the case of a pure resistive load the only loss of stability of the in-phase periodic solutions to asymmetric perturbations is by a period-doubling bifurcation. Our more detailed numerical studies confirm the occurence of the period-doubling bifurcation and also show the existence of fixed-point bifurcations (albeit for a very small parameter range). The bifurcation curves are shown in figure 9. We integrated a variety of initial conditions near the period-doubling bifurcation, finding period-doubled solutions that were in accord with the theoretical predictions of sections 3 and 4. In particular, when $N = 5$ we found a period-doubling bifurcation, as I was decreased, at $\beta = 2$ and $I \simeq 1.6$. Some of these results are tabulated in table 1. It is worth pointing out that we did *not* make a coherent organized search in parameter space for different phenomena.

We note that as we varied the parameters quasistatically away from the curve of period-doubling bifurcations in the (β, I)-plane, we found secondary bifurcations to more complicated block structures of oscillators whose existence and/or asymptotic stability was not predicted by our local theory. This was not a surprise. Finally, we did *not* find any evidence for primary branches of stable period-doubled solutions with submaximal symmetry, which would have been allowed by local theory. For moderate and large values of beta we also found another type of global solution. In

Table 1. Numerical simulation results for pure resistive load.

					Initial conditions (φ, $\dot{\varphi}$)		
N	β	I	Isotropy	Stability	Block 1	Block 2	Block 3
4	1.0	1.6	T_2	yes	1.41, 0.11	1.30, 0.63	——
5	2.0	1.55	Σ_2	yes	2.75, 0.39	3.34, 0.68	——
5	2.0	1.5	T_2	no	4.53, 1.11	2.99, 0.40	3.76, 0.77
5	2.0	1.55	Σ_1	no	0.60, 0.88	5.74, 1.13	——
13	2.0	1.55	Σ_6	yes	3.94, 0.91	3.09, 0.50	——
2	1.5	1.01	T_1†	yes	1.27, 0.072	1.44, −0.021	——
2	5.0	0.9	Semirotor	yes	4.64, 0.73	0.86, −0.01	——

† In systems with two oscillators T_1 solutions have the same symmetry as POMS.

these solutions, which we call *semirotors,* there are two groups of junctions with the junctions within each group in phase with one another. In one group the junctions all follow a running waveform (i.e., a solution which is periodic on a cylinder) while in the other group they all execute a simple periodic motion. Semirotors are discussed in more detail in [1].

6.2. *Capacitive load*

We integrated the second-order system (2.7) by writing it as a first-order system:

$$\dot{\varphi}_k = \psi_k \tag{6.2a}$$

$$\dot{\psi}_k = \frac{1}{3+\beta} I - \frac{1}{\beta}\left(\psi_k + \sin(\varphi_k) - \frac{3}{N(3+\beta)} \sum_{j=1}^{N} [\psi_j + \sin(\varphi_j)]\right) \tag{6.2b}$$

for $k = 1, \ldots, N$.

As noted in section 2.2, see figure 6, the in-phase periodic solutions are born at homoclinic bifurcations and lose stability both by period doubling and fixed-point bifurcations. Since theory predicts that the fixed-point bifurcations should lead to unstable asymmetric solutions, it is not surprising that we found no local bifurcation dynamics at this transition. More surprising, perhaps, is that no asymptotically stable period-doubled solutions were observed at these transitions, though this is 'allowed' by theory. Instead of stable period doubled solutions we found semirotors (described in section 6.1) and discrete rotating waves (described below).

We did experiment with initial conditions inside fixed-point subspaces and this did lead to the predicted fixed-point and period-doubled oscillator groupings. Some of our results are presented in table 2.

The codimension-two point (labelled P) where curves of period-doubling and fixed-point bifurcation terminate along the curve of homoclinic bifurcations is shown in figure 6. This point is discussed in the next section.

In our numerical exploration of the capacitive load model we found discrete rotating wave solutions whose existence could not have been predicted by local bifurcation theory in this system. We call these solutions *ponies on a merry-go-*

Table 2. Numerical simulation results for capacitive load; all period-doubled and fixed point solutions are unstable.

					Initial conditions		
N	β	I	Isotropy	Bifurcation	Block 1	Block 2	Block 3
4	0.7	1.4	Σ_1	per-dbl	2.13, 0.49	2.18, 0.52	——
5	0.7	0.8	Σ_1	per-dbl	4.75, 0.96	4.38, 0.82	——
5	0.9	0.8	Σ_2	per-dbl	1.72, −0.22	3.00, 0.37	——
5	0.3	0.9	Σ_2	fixed-pt	6.06, 0.96	5.57, 1.32	——
3	0.1	1.2	POM	stable	2.11, 0.33	6.08, 1.56	1.34, 0.23
3	0.1	1.02	per-dbl POM	stable	1.73, 0.41	1.92, 0.44	1.40, 0.42
3	0.1	0.99	torus	stable	2.49, 0.24	3.01, 0.67	1.77, −0.12
6	0.1	1.2	POM in groups of two	unstable	1.36, 0.27	6.23, 1.45	2.15, 0.39
2	3.0	0.64	semirotor	stable	2.49, 0.12	1.29, −0.01	——

round or POMs. More precisely, an N-oscillator POM is a period-T solution in which each oscillator traverses the same trajectory in phase space and the oscillators can be ordered so that each oscillator is T/N out of phase with the previous oscillator. Of course, POMs can be formed with groups of oscillators rather than with single oscillators. We have observed POMs with non-trivial groupings, but only with initial conditions in particular fixed-point subspaces. These POMs appear to be asymptotically unstable. Several entries in table 2 indicate parameter values where POMs have been found.

POM solutions can be found by solving a differential delay equation in the plane as follows. Order the oscillators and search for T-periodic solutions of the form:

$$(\varphi_1(t), \varphi_2(t), \varphi_3(t), \ldots) = (\varphi(t), \varphi(t-\tau), \varphi(t-2\tau), \ldots)$$

where the delay $\tau = T/N$. Such a delay equation is unusual since we search for periodic solutions whose period is coupled to the delay. Using topological degree methods it is possible to prove the existence of POMs in both the resistive and the capacitive load models whenever $I > 1$. See the companion paper [3] for this proof. Asymptotic stability is not considered by this method. Tracking along branches of POMs leads to an interesting bifurcation whose theoretical analysis is found in Fiedler [7]. To describe this bifurcation requires a short diversion into the theory of periodic solutions in symmetric systems.

Consider a system of ODE with symmetry group Γ and periodic solution $x(t)$. There are two subgroups of Γ related to $x(t)$:

$$K = \{\gamma \in \Gamma : \gamma x(t) = x(t) \quad \text{for all } t\} \tag{6.3a}$$

$$H = \{\gamma \in \Gamma : \gamma\{x(t)\} = \{x(t)\}\}. \tag{6.3b}$$

K is the subgroup of *spatial* symmetries of $x(t)$ and H is the subgroup of *spatial–temporal* of x. To see this note that $h \in H$ maps the trajectory of x onto itself. Hence, by uniqueness of solutions, there is a phase shift θ such that:

$$hx(t) \equiv x(t-\theta). \tag{6.4}$$

For the POM solutions discussed above $H = S_N$ and $K = \{1\}$.

Let S be a cross-section to the periodic solution x. S can be chosen to be K-invariant. Let P be the associated Poincaré map. Uniqueness of solutions to systems of ODE implies that P commutes with K; it is less clear what effects the symmetries H have on P. Roughly speaking, Fiedler's observation is that if $[H/K] = m$ is finite then $P = Q^m$, where Q is the $1/m$th period map obtained by integrating the ODE. There is a simple consequence of this observation for generic bifurcations of P, since

$$(\mathrm{d}P)_{x(0)} = (\mathrm{d}Q)^m_{x(0)}.$$

Thus, when m is even and $\mathrm{d}Q$ has -1 as an eigenvalue, then $\mathrm{d}P$ will have $+1$ as an eigenvalue.

We have observed such a bifurcation of POMs. Period-doubling of Q leads to a pitchfork-type bifurcation of fixed points for P when m is even (that is, to non-POM asymmetric period orbits for the original system of ODE) and to a period-doubling bifurcation for P when m is odd (that is, to a period-doubled POM for the original system of ODE). This bifurcation was detected numerically at:

$$N = 3 \qquad I \simeq 1.172 \qquad \beta = 0.1. \tag{6.5}$$

We also note that a bifurcation to invariant tori off the period-doubled POMs was observed when

$$N = 3 \qquad I = 0.992 \qquad \beta = 0.1. \tag{6.6}$$

Finally we note that there is numerical evidence that the POM solutions disappear (at some $I < 1$) through a heteroclinic bifurcation indicating that the complete dynamics of this system is far from understood.

7. Homoclinic twist points and a new codimension-two bifurcation

In our numerical studies of Josephson junction arrays with a pure capacitive load we have observed a new codimension-two bifurcation where, in parameter space, a curve of period doubling bifurcations and a curve of fixed point bifurcations terminate simultaneously on the curve Γ of homoclinic orbits along which the in-phase rotations are born. This bifurcation occurs at the point labelled P in figure 6. The point P is a *homoclinic twist point,* i.e., as the parameter point passes through P on Γ there is a change in orientation in the tangent flow over the homoclinic orbit. In subsection 7.1 we show that homoclinic twist points occur for both resistive and capacitive loads. Indeed, our numerical studies show that in the capacitive load case the homoclinic twist point is unique, while in the resistive load case there are three of them. A homoclinic twist point will be called a *homoclinic twist bifurcation point* if there are bifurcation curves emanating from it. In subsection 7.2 we explain why the unique homoclinic twist point in the capacitive load case is also a bifurcation point. However, as we will see in subsection 7.3 where we discuss the resistive load case, a homoclinic twist point is not necessarily a bifurcation point.

7.1. Homoclinic twist points

The occurrence of homoclinic twist points is independent of the number N of junctions in the array. We therefore restrict our attention to the simplest case $N = 2$. Set

$$r \equiv \tfrac{1}{2}(\varphi_1 - \varphi_2) \qquad s \equiv \tfrac{1}{2}(\varphi_1 + \varphi_2).$$

Then for a resistive load r and s satisfy

$$\begin{aligned} &\beta \ddot{r} + \dot{r} + \sin(r)\cos(s) = 0 \\ &\beta \ddot{s} + 2\dot{s} + \sin(s)\cos(r) = I \end{aligned} \tag{7.1 res}$$

while for a capacitive load r and s satisfy

$$\begin{aligned} &\beta \ddot{r} + \dot{r} + \sin(r)\cos(s) = 0 \\ &(3+\beta)\ddot{s} + \dot{s} + \sin(s)\cos(r) = I. \end{aligned} \tag{7.1 cap}$$

Note that the r-equation is the same in both systems.

The invariant subspace (plane) of in-phase solutions is

$$S \equiv \{(r, \dot{r}, s, \dot{s}) \in \mathbb{R}^4 : r = \dot{r} = 0\}.$$

For $I<1$, both of the systems (7.1) have two rest points in S given by

$$r=\dot{r}=\dot{s}=0 \qquad s=\begin{cases}\sin^{-1}(I)\\ \pi\text{-}\sin^{-1}(I).\end{cases}$$

The point $\mathcal{P}(I)\equiv(0,0,\pi\text{-}\sin^{-1}(I),0)$ is hyperbolic. The differential of either of the systems (7.1) evaluated at $\mathcal{P}(I)$ has a stable and an unstable eigendirection in S, as well as a stable and unstable eigendirection transverse to S in $\mathbb{R}^4\backslash S$. For $I=1$, $\mathcal{P}(1)=(0,0,\pi/2,0)$ is a non-hyperbolic rest point. The differentials of the system (7.1) at $\mathcal{P}(1)$ have a stable and a center unstable eigendirection in S, as well as a stable and center unstable eigendirection in $\mathbb{R}^4\backslash S$. For the flow restricted to S, the stable and unstable or centre unstable manifolds coincide for $(I,\beta)\in\Gamma$, i.e., for $I=I(\beta)$. We will use the notation $\mathcal{P}(\beta)\equiv\mathcal{P}(I(\beta))$.

For any parameter point on Γ, let

$$\sigma(\cdot;\beta)\equiv(0,0,\varphi(\cdot;\beta),\dot{\varphi}(\cdot;\beta))$$

denote the homoclinic orbit in S. Then $\sigma(t;\beta)\to\mathcal{P}(\beta)$ as $t\to\pm\infty$. As we have seen in section 2, the variational system along the symmetric orbit $\sigma(\cdot;\beta)$ is partially uncoupled into two two-dimensional subsystems, one over S and the other over $\mathbb{R}^4\backslash S$. The variational subsystem over $\mathbb{R}^4\backslash S$ is given by

$$\dot{X}=B(t;\beta)X \tag{7.2}$$

where

$$B(t;\beta)=\frac{1}{\beta}\begin{pmatrix}0 & \beta\\ -\cos\varphi(t;\beta) & -1\end{pmatrix}.$$

To study the tangent flow, we introduce polar coordinates

$$X=\begin{pmatrix}\rho\cos(\theta)\\ \rho\sin(\theta)\end{pmatrix}$$

so that the system (7.2) becomes

$$\frac{\dot{\rho}}{\rho}=\left(1-\frac{1}{\beta}\cos(\varphi)\right)\sin(\theta)\cos(\theta)-\frac{1}{\beta}\sin^2(\theta) \tag{7.3a}$$

$$\dot{\theta}=-\sin^2(\theta)-\frac{1}{\beta}\sin(\theta)\cos(\theta)-\frac{1}{\beta}\cos(\varphi)\cos^2(\theta). \tag{7.3b}$$

Note that equation (7.3b) is independent of ρ, so that given the homoclinic orbit $\sigma(\cdot;\beta)$ we can analyse the angular evolution of the restriction of the tangent flow to $\mathbb{R}^4\backslash S$ simply by studying the dynamics of (7.3b).

The $\dot{\theta}$-null clines of (7.3b) are given by

$$\sin^2(\theta)+\frac{1}{\beta}\sin(\theta)\cos(\theta)+\frac{1}{\beta}\cos\varphi\cos^2(\theta)=0 \tag{7.4}$$

Since the left-hand side of (7.4) is equal to 1 when θ is any odd multiple of $\pi/2$, we can divide both sides by $\cos^2(\theta)$ to obtain

$$\tan^2(\theta)+\frac{1}{\beta}\tan(\theta)+\frac{1}{\beta}\cos(\varphi)=0.$$

Therefore the equations for the $\dot{\theta}$-null clines are

$$\tan(\Theta^{\pm}(\cdot;\beta)) = \frac{1}{2\beta}\{-1 \pm \sqrt{1-4\beta\cos(\varphi(\cdot;\beta))}\} \tag{7.5}$$

As $t \to \pm\infty$, $\varphi(t;\beta) \to \bar{\varphi}(\beta) \equiv \pi\text{-}\sin^{-1}(I(\beta))$. Thus

$$\tan(\theta^{\pm}(t;\beta)) \to \frac{1}{2\beta}\{-1 \pm \sqrt{1+4\beta\zeta}\}$$

as $t \to \pm\infty$, where

$$\zeta \equiv \sqrt{1-I^2(\beta)}.$$

Set $\Theta^{\pm}(\beta) \equiv \Theta^{\pm}(\pm\infty;\beta)$. It is easy to verify that $\tan(\Theta^{+}(\beta))$ is the slope of the unstable or centre unstable eigendirection and $\tan(\Theta^{-}(\beta))$ is the slope of the stable eigendirection for

$$B(\pm\infty;\beta) = \frac{1}{\beta}\begin{pmatrix} 0 & \beta \\ \zeta & -1 \end{pmatrix}.$$

If $\beta < \frac{1}{4}$ then the $\dot{\theta}$-null clines $\theta = \Theta^{\pm}(t;\beta)$ and all their translates by multiples of π are defined for all $t \in \mathbb{R}$. The θ-flow given by (7.3*b*) is as shown in figure 10(*a*). For convenience, in the figure we have drawn θ as a function of φ on the interval $[\bar{\varphi}, \bar{\varphi}+2\pi]$. This is permissible since, in view of the constructions described in section 2, along the symmetric homoclinic orbit $\dot{\varphi}(\cdot;\beta) > 0$ on $(\bar{\varphi}, \bar{\varphi}+2\pi)$. There is a unique orbit $\theta = \theta_1(\cdot;\beta)$ such that

$$\theta_1(t;\beta) \to \Theta^{+}(\beta) \qquad \text{as } t \to \pm\infty$$

and a unique orbit $\theta = \theta_2(\cdot;\beta)$ such that

$$\theta_2(t;\beta) \to \Theta^{-}(\beta) \qquad \text{as } t \to \pm\infty.$$

For all other orbits $\theta = \theta(\cdot;\beta)$ which lie between $\theta = \theta_2$ and $\theta = \theta_2 + \pi$ we have

$$\theta(t;\beta) \to \begin{cases} \Theta^{-}(\beta)(\text{mod } \pi) & \text{as } t \to -\infty \\ \Theta^{+}(\beta) & \text{as } t \to +\infty. \end{cases}$$

For $\beta \gg 1$,

$$\tan\Theta^{\pm}(t;\beta) \sim \pm\sqrt{\zeta/\beta} \qquad \text{as } t \to \pm\infty$$

and outside the $\dot{\theta}$-null clines the θ-flow is approximated by

$$\dot{\theta} = -\sin^2(\theta).$$

From these observations it is not difficult to verify that the θ-flow is as shown in figure 10(*c*). In particular for $\beta \gg 1$ there are no orbits which satisfy $\theta(t;\beta) \to \Theta^{+}(\beta)$ as $t \to \pm\infty$ or $\theta(t;\beta) \to \Theta^{-}(\beta)$ as $t \to \pm\infty$. Instead, there is a unique orbit $\theta = \theta_1(\cdot;\beta)$ such that

$$\theta_1(t;\beta) \to \begin{cases} \Theta^{+}(\beta) & \text{as } t \to -\infty \\ \Theta^{+}(\beta) - \pi & \text{as } t \to +\infty \end{cases}$$

and a unique orbit $\theta = \theta_2(\cdot;\beta)$ such that

$$\theta_2(t;\beta) \to \begin{cases} \Theta^{-}(\beta) & \text{as } t \to -\infty \\ \Theta^{-}(\beta) - \pi & \text{as } t \to +\infty. \end{cases}$$

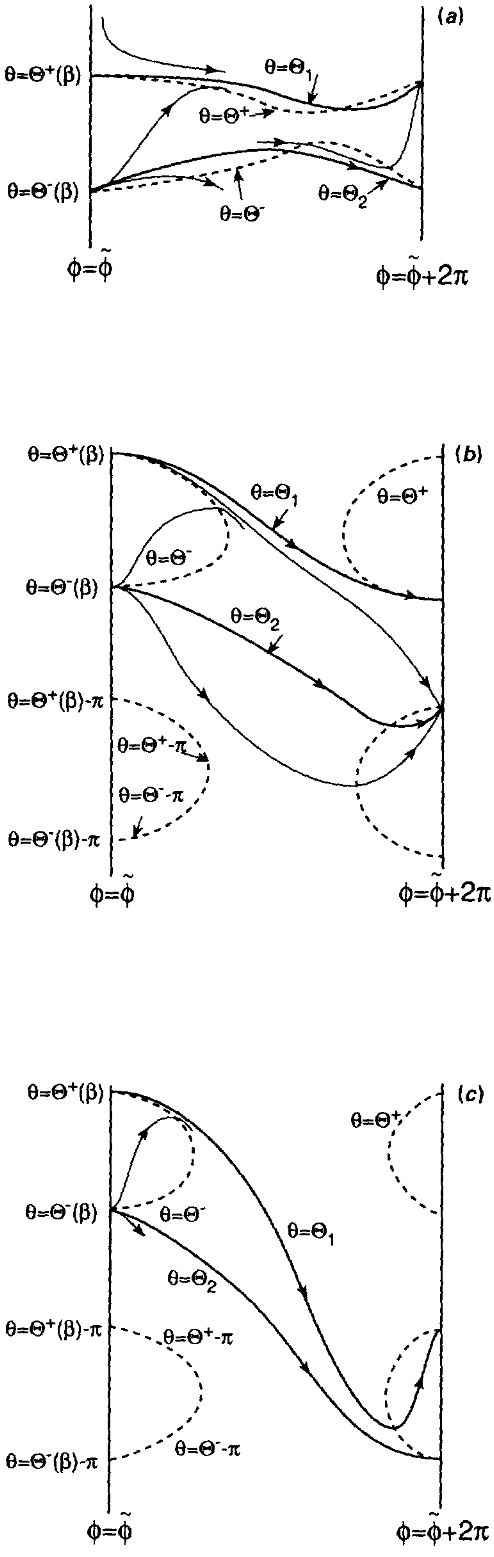

Figure 10. The θ-flow for various values of β. (a) $\beta < 1/4$. (b) $\beta = \beta^*$, a homoclinic 1-twist point. (c) $\beta \gg 1$.

Thus the θ-flow for $\beta \gg 1$ is twisted by $-\pi$ radians in comparison to the θ-flow for $\beta < 1/4$.

For any solution $\theta = \theta(\cdot; \beta)$ to (7.3*b*) we have

$$\theta(t; \beta) \to \Theta^{\pm}(\beta) + k\pi$$

for some choice of sign and some choice of $k \in \mathbb{Z}$ both as $t \to -\infty$ and as $t \to +\infty$. Given $k \in \mathbb{N}$ we call a point $(I(\beta^*), \beta^*)$ a *homoclinic k-twist point* if there exists an orbit $\theta = \theta_1(\cdot; \beta^*)$ such that

$$\theta_1(t; \beta^*) \to \begin{cases} \Theta^+(\beta) & \text{as } t \to -\infty \\ \Theta^-(\beta) - (k-1)\pi & \text{as } t \to +\infty \end{cases}$$

and an orbit $\theta = \theta_2(\cdot; \beta^*)$ such that

$$\theta_2(t; \beta^*) \to \begin{cases} \Theta^-(\beta) & \text{as } t \to -\infty \\ \Theta^+(\beta) - k\pi & \text{as } t \to +\infty \end{cases}.$$

That is, for $\beta = \beta^*$ the θ-flow carries the unstable or centre unstable eigendirection in $\mathbb{R}^4 \backslash S$ at $\mathscr{P}(\beta^*)$ into the stable eigendirection in $\mathbb{R}^4 \backslash S$ at $\mathscr{P}(\beta^*)$ after a twist of $-(k-1)\pi$ radians. Similarly, the stable eigendirection in $\mathbb{R}^4 \backslash S$ at $\mathscr{P}(\beta^*)$ is carried into the corresponding unstable or centre unstable eigendirection after a twist of $-k\pi$ radians. It is clear that in the transition from the configuration for small β shown in figure 10(*a*) to the configuration for large β shown in figure 10(*c*) there must be at least one value of β, say β^*, for which $(I(\beta^*), \beta^*)$ is a homoclinic 1-twist point as shown in figure 10(*b*).

In the case of a capacitive load, our numerical studies show that there is a unique homoclinic 1-twist point (labelled P in figure 6) and no other twist points for $k \neq 1$. In the case of a resistive load our numerical studies show that there are exactly three isolated homoclinic twist points (labelled P_j in figure 9). The P_j have coordinates $(1, \beta_j^*)$ where

$$\beta_1^* \in (0.3, 0.4) \qquad \beta_2^* \in (0.5, 0.6) \qquad \beta_3^* \in (2.05, 2.1).$$

Points P_1 and P_3 are homoclinic 1-twist points, while P_2 is a homoclinic 2-twist point.

7.2. *Homoclinic twist bifurcation in the capacitive load case*

Let $\sigma(\cdot; I, \beta) \equiv (0, 0, \varphi(\cdot; I, \beta), \dot{\varphi}(\cdot; I, \beta))$ denote the (unique) symmetric running solution to either of the systems (7.1) for $I > I(\beta)$ and $\beta > 0$. As we observed in section 2, the stability of this solution depends on the Floquet multipliers $\mu_1(I, \beta)$ and $\mu_2(I, \beta)$ associated with the two-dimensional variational subsystem

$$\dot{X} = \frac{1}{\beta} \begin{pmatrix} 0 & \beta \\ -\cos(\varphi(t; I, \beta)) & -1 \end{pmatrix} X \tag{7.6}$$

and that only fixed point or period doubling bifurcations are possible. Let $X(\cdot; I, \beta)$ denote the fundamental matrix solution to (7.6), i.e., the solution with $X(0) = I$. Then μ_1 and μ_2 are the eigenvalues of $X(I, \beta) \equiv X(T(I, \beta); I, \beta)$, where $T(I, \beta)$ is the period of σ. It is well known that, modulo a transversality condition, fixed point bifurcations occur when

$$\operatorname{tr} X(I, \beta) = 1 + \mathrm{e}^{-T/\beta} \tag{7.7a}$$

and period doubling bifurcations occur when

$$\operatorname{tr} X(I, \beta) = -(1 + e^{-T/\beta}). \tag{7.7b}$$

In terms of the polar coordinates introduced in section 7.1,

$$\operatorname{tr} X(I, \beta) = \rho_0(I, \beta) \cos(\theta_0(I, \beta)) + \rho_{\pi/2}(I, \beta) \sin(\theta_{\pi/2}(I, \beta)). \tag{7.8}$$

Here $\rho_*(I, \beta) \equiv \rho_*(T(I, \beta); I, \beta)$ and $\theta_*(I, \beta) - \theta_*(T(I, \beta); I, \beta)$, where θ_* is the solution to

$$\dot{\theta}_* = -\sin^2(\theta) - \frac{1}{\beta} \sin(\theta) \cos(\theta) - \frac{1}{\beta} \cos(\varphi) \cos^2(\theta)$$

$$\theta(0) = *$$

ρ_* is the solution to

$$\frac{\dot{\rho}}{\rho} = \left(1 - \frac{1}{\beta} \cos(\varphi)\right) \sin(\theta_*) \cos(\theta_*) - \frac{1}{\beta} \sin^2(\theta_*)$$

$$\rho(0) = 1$$

and $* = 0$ or $\pi/2$.

In the capacitive load case there is a unique homoclinic 1-twist point P with coordinates $(I(\beta^*), \beta^*)$. For $\beta > \beta^*$

$$\lim_{I \downarrow I(\beta)} \theta_*(I, \beta) = \Theta^+(\beta) - \pi$$

while for $\beta \in (0, \beta^*)$

$$\lim_{I \downarrow I(\beta)} \theta_*(I, \beta) = \Theta^+(\beta).$$

Moreover, it can be shown that for any $\beta > 0$

$$\lim_{I \downarrow I(\beta)} \rho_*(I, \beta) = +\infty$$

(cf [2]). Hence it follows from (6.8) that

$$\lim_{I \downarrow I(\beta)} \operatorname{tr} X(I, \beta) = \begin{cases} +\infty & \text{if } \beta < \beta^* \\ -\infty & \text{if } \beta > \beta^*. \end{cases}$$

For arbitrary β_1 and β_2 satisfying $0 < \beta_1 < \beta^* < \beta_2$ consider an arc $\mathscr{C}$ lying wholly to the right of Γ and joining $K_1 \equiv (I(\beta_1), \beta_1)$ to $K_2 \equiv (I(\beta_2), \beta_2)$. For points near K_1 on $\mathscr{C}$

$$\operatorname{tr} X(I, \beta) \ll -2 \leqslant -(1 + e^{-T/\beta})$$

and for points near K_2 on $\mathscr{C}$

$$\operatorname{tr} X(I, \beta) \gg 2 \geqslant 1 + e^{-T/\beta}.$$

Since $\operatorname{tr} X(I, \beta)$ is continuous on $\mathscr{C}$ it follows that there exist points on $\mathscr{C}$ where (7.7*a*) and (7.7*b*) hold, i.e., fixed point and period doubling bifurcation points. This proves the existence of bifurcations arbitrarily close to the homoclinic twist point P. Further argument is needed to show that there are curves of fixed point and period doubling bifurcation emanating from P as indicated by our computations. For this the reader is referred to [2].

Fiedler has observed that an index argument similar to those given in [7] implies the existence of another curve of homoclinic orbits emanating from the homoclinic twist bifurcation point P. A formal analysis in the case $N = 2$ suggests that the homoclinic orbits on this curve are double homoclinic loops through $\mathscr{P}(\beta^*)$ in $\mathbb{R}^4 \backslash S$ ('bellows'). An analysis of these homoclinic loops will appear in [2].

7.3. The resistive load case

If $P \in \Gamma$ is a homoclinic twist point then, by the argument given in subsection 7.2, P is a homoclinic twist bifurcation point if

$$\inf|\mathrm{tr}\, X(I, \beta)| > 1$$

in some neighbourhood of P. On the other hand, P is not a homoclinic twist bifurcation point if

$$\sup|\mathrm{tr}\, X(I, \beta)| < 1 \tag{7.9}$$

in some neighbourhood of P.

Our numerical studies show that (7.9) holds for each of the three homoclinic twist points P_j ($j = 1, 2, 3$) in the resistive load case. Thus we conclude that the P_j are not homoclinic twist bifurcation points. Figure 11 shows the computed values of $\mathrm{tr}\, X(\cdot, 1.00001)$ for $\beta \in (0, 2.2)$. For more details refer to [2].

Even though there are no homoclinic twist bifurcations in the resistive load case, there are nevertheless bifurcation points on the segment of Γ with $\beta \in (0, \hat{\beta})$. These points are shown in figure 9 along with the curve γ^+ of fixed point bifurcations and the curve γ^- of period doubling bifurcations. These curves represent our best current knowledge of the complete bifurcation picture. They were computed using

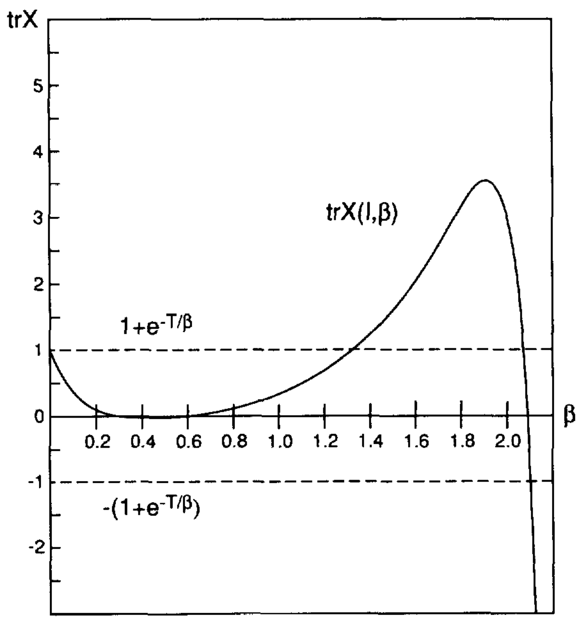

Figure 11. $\mathrm{tr}\, X(I, \beta)$ against β for $I = 1.00001$.

AUTO and verified by various other numerical techniques. There is some uncertainty due to the smallness of the interval (β_2^+, β_1^-). Although we believe that this interval has positive length, further study may show its length to be zero in which case the homoclinic twist point P_3 will be promoted to a homoclinic twist bifurcation point.

Acknowledgment

We are grateful to Kurt Wiesenfeld for pointing out a number of the interesting symmetry features of the arrays of Josephson junctions and to Eusebius Doedel for computing the bifurcation diagrams using AUTO. We also wish to thank Bernold Fiedler, Pascal Chossat, Mike Field and Ian Melbourne for helpful discussions.

The research of DGA was supported in part by NSF grant DMS-8905456. The research of MG was supported in part by NSF/DARPA grant (DMS-8700897) and by the Texas Advanced Research Program under Grant ARP-1100. The research of MK was supported in part by the Air Force and NSF through a postdoctoral fellowship at the Institute for Mathematics and Applications.

References

[1] Aronson D G 1991 Semirotors in Josephson junction arrays, in preparation

[2] Aronson D G, Fiedler B, Jolly M and Krupa M 1991 Homoclinic twist points and bifurcations, in preparation

[3] Aronson D G, Golubitsky M and Mallet-Paret J 1991 Ponies on a merry-go-round in large arrays of Josephson junctions *Nonlinearity* **4** 903–10

[4] Buchner M, Marsden J and Schecter S 1983 Applications of the blowing-up construction and algebraic geometry to bifurcation problems *J. Diff. Eq.* **48** 404–33

[5] Chossat P and Golubitsky M 1988 Iterates of maps with symmetry *SIAM J. Math. Anal.* **19** 1259–70

[6] Chossat P and Golubitsky M 1988 Symmetry increasing bifurcations of chaotic attractors *Physica* **32D** 423–36

[7] Fiedler B 1988 Global Bifurcation of Periodic Solutions with Symmetry *Lecture Notes on Mathematics* **1309** (Berlin: Springer)

[8] Field M and Richardson R W 1989 Symmetry breaking and the maximal isotropy subgroup conjecture for reflection groups. Arch. Rat. Mech. Anal. **105** 61–94

[9] Golubitsky M and Schaeffer D G 1985 *Singularities and Groups in Bifurcation Theory: Vol. I,* (*Appl. Math. Sci. Ser.* **51** (Berlin: Springer))

[10] Golubitsky M, Stewart I N and Schaeffer D G 1988 *Singularities and Groups in Bifurcation theory: Vol. II* (*Appl. Math. Sci. Ser* **69** (Berlin: Springer))

[11] Hadley P 1989 Dynamics of Josephson Junction Arrays *Thesis* Department of Applied Physics, Stanford University

[12] Hadley P, Beasley M R and Wiesenfeld K 1988 Phase locking of Josephson-junction series arrays *Phys. Rev. B* **38** 8712–19

[13] Hadley P, Beasley M R and Wiesenfeld K 1988 Phase locking of Josephson junction arrays *Appl. Phys. Lett.* **52** 1619–21.

[14] Ihrig E and Golubitsky, M 1984 Pattern selection with O(3) symmetry *Physica* **12D** 1–33

[15] McLeod B and Sattinger D H 1973 Loss of stability and bifurcation at a double eigenvalue *J. Func. Anal.* **14** 62–84

[16] Schecter S 1987 The saddle-node separatrix-loop bifurcation, *SIAM J. Math. Anal.* **18** 1142–56

[17] Tsang K Y, Mirollo R E, Strogatz S H and Wiesenfeld K 1991 Dynamics of a globally coupled oscillator array *Physica* D in press